Published in final edited form as:
Nature. 2018 March 15; 555(7696): 382–386. doi:10.1038/nature25974.

Recognition of DHN-melanin by MelLec, is required for protective immunity to *Aspergillus*

Mark H.T. Stappers[#a], **Alexandra E. Clark**[#a], **Vishukumar Aimanianda**[#b], **Stefan Bidula**[a], **Delyth M. Reid**[a], **Patawee Asamaphan**[a], **Sarah E. Hardison**[a], **Ivy M. Dambuza**[a], **Isabel Valsecchi**[b], **Bernhard Kerscher**[a], **Anthony Plato**[a], **Carol A. Wallace**[a], **Raif Yuecel**[c], **Betty Hebecker**[a], **Maria da Glória Teixeira Sousa**[a], **Cristina Cunha**[d], **Yan Liu**[e], **Ten Feizi**[e], **Axel A. Brakhage**[f], **Kyung J. Kwon-Chung**[g], **Neil A. R. Gow**[a], **Matteo Zanda**[a,$], **Monica Piras**[a,$], **Chiara Zanato**[a,$], **Martin Jaeger**[h], **Mihai G. Netea**[h], **Frank L. van de Veerdonk**[h], **João F. Lacerda**[i], **António Campos Jr.**[j], **Agostinho Carvalho**[d], **Janet A. Willment**[a], **Jean-Paul Latgé**[b,k], and **Gordon D. Brown**[a,*]

[a]Medical Research Council Centre for Medical Mycology at the University of Aberdeen, Aberdeen Fungal Group, Foresterhill, Aberdeen, AB25 2ZD, UK [$]Institute of Medical Sciences, University of Aberdeen, Foresterhill, Aberdeen, AB25 2ZD, UK [b]Unité des Aspergillus, Institut Pasteur, Paris, France [c]Iain Fraser Cytometry Centre, Institute of Medical Sciences, University of Aberdeen, Aberdeen, AB25 2ZD, UK [d]Life and Health Sciences Research Institute (ICVS), School of Medicine, University of Minho, and ICVS/3B's - PT Government Associate Laboratory, Braga/ Guimarães, Portugal [e]Glycosciences Laboratory, Department of Medicine, Imperial College London, London, W12 0NN, UK [f]Department of Microbiology and Molecular Biology, Leibniz Institute for Natural Product Research and Infection Biology (HKI), Friedrich Schiller University, D-07745 Jena, Germany [g]Molecular Microbiology Section, Laboratory of Clinical Immunology and Microbiology, National Institute of Allergy and Infectious Diseases (NIAID), National Institutes of Health (NIH), Bethesda, Maryland, United States of America [h]Department of Internal Medicine, Radboud University Medical Center, Nijmegen, The Netherlands [i]Instituto de Medicina Molecular, Faculdade de Medicina de Lisboa, Lisboa, Portugal; and Serviço de Hematologia e

[*]Correspondence and requests for materials should be addressed to GDB (gordon.brown@abdn.ac.uk).
[k]Present address: State Key Laboratory, Institute of Microbiology, Chinese Academy of Sciences, Beijing, China.

Author contributions

GDB, JPL and JAW conceived and designed the study and guided the interpretation of the results. AEC, MHTS, and VA performed the majority of the experiments and data analysis. SB, DMR, PA, SEH, ID, BK, AP, JAW, CC, MGS, CW, RY, BH conducted experiments and data analysis. YL and TF performed the glycan microarray experiments and data analysis. MJ, MN, FLvdV, JFL, AC Jr and AC provided the human patient data and analysis. AAB, KJK, IV, MP, CZ, MZ and NG provided critical conceptual input and reagents. GDB drafted the manuscript. All authors discussed the results, edited and approved the draft and final versions of the manuscript.

Author Information

Reprints and permissions information is available at www.nature.com/reprints.

The authors declare no competing financial interests.

Data availability

The data that support the findings of this study are available from the corresponding author upon reasonable request.

Europe PMC Funders Author Manuscripts

Transplantação de Medula, Hospital de Santa Maria, Lisboa, Portugal [j]Serviço de Transplantação de Medula Óssea (STMO), Instituto Português de Oncologia do Porto, Porto, Portugal

[#] These authors contributed equally to this work.

Abstract

Our resistance to infection is critically dependent upon the ability of pattern recognition receptors to recognise microbial invasion and induce protective immune responses. One such family of receptors are the C-type lectins, which play central roles in antifungal immunity1. These receptors activate key effector mechanisms upon recognition of conserved fungal cell wall carbohydrates. However, several other immunologically active fungal ligands have been described, including melanin2,3, whose mechanisms of recognition remain largely undefined. Here we identify a C-type lectin receptor, Melanin sensing C-type Lectin receptor (MelLec), that plays an essential role in antifungal immunity through recognition of the naphthalene-diol unit of 1,8-dihydroxynaphthalene (DHN)-melanin. MelLec recognises melanin in conidial spores of *Aspergillus fumigatus*, as well as other DHN-melanised fungi and is ubiquitously expressed by $CD31^{+}$ endothelial cells in mice. MelLec is also expressed by a sub-population of these cells in mice that co-express EpCAM and which were detected only in the lung and liver. In mouse models, MelLec was required for protection against disseminated infection with *A. fumigatus*. In humans, MelLec is also expressed by myeloid cells, and we identified a single nucleotide polymorphism of this receptor that negatively affected myeloid inflammatory responses and significantly increased susceptibility of stem-cell transplant recipients to disseminated *Aspergillus* infections. Thus MelLec is a receptor recognising an immunologically active component commonly found on fungi and plays an essential role in protective antifungal immunity in both mice and humans.

C-type lectin receptors (CLRs) involved in antifungal immunity belong primarily to the Dectin-1 and Dectin-2 clusters of receptors located near the Natural Killer Gene complex (NKC)1. To identify new CLRs within these clusters that recognise fungi, we generated soluble protein chimeras consisting of the C-type lectin-like domain (CTLD) of murine receptors fused to the Fc region of human IgG14 (Fc-MelLec, Extended data Fig. 1a) and used these chimeric proteins as probes to screen for recognition of fungi by flow cytometry. Using this approach, we identified the CTLD of MelLec (*CLEC1A*5, Extended data Fig. 1b), which bound *Aspergillus fumigatus* conidia (Fig. 1a). MelLec did not recognise other commonly occurring fungi, such as *Candida albicans* yeast and filamentous cells or *Saccharomyces cerevisiae* yeasts, but did recognise other melanised fungal species, including *Fonsecaea pedrosoi* and *Cladosporium cladosporioides* (Fig. 1b, Extended data Fig. 1c,e). This indicated that the ligand recognised by MelLec was not ubiquitously found in all fungi, unlike the ligands of other anti-fungal CLRs, such as Dectin-11. Notably, the ability of MelLec to recognise *A. fumigatus* was restricted to conidia, and recognition was rapidly lost following conidial swelling, germination and hyphal growth (Fig. 1a,c and Extended data Fig. 2d). Visualising binding to conidia by immunofluorescence microscopy, revealed a punctate staining pattern suggestive of restricted distribution of the moiety recognised by MelLec on these spores (Fig. 1c). Conidia are covered by a hydrophobic

rodlet layer which masks underlying cell wall components from immune recognition6. Removal of this rodlet layer with NaOH6 led to increased and uniform binding of MelLec over the entire conidial surface (Fig. 1d). Indeed, uniform staining was obtained with rodlet-deficient conidia (Δ*rodA*), confirming that the ligand of MelLec was being partially masked by the surface hydrophobin layer (Fig. 1e). Recognition of *A. fumigatus* conidia by MelLec could also be demonstrated in a cellular context using MelLec reporter cells4 (Extended data Fig. 1f).

All characterised CLRs involved in fungal sensing recognise carbohydrate components of the fungal cell wall1. Consistent with this possibility, MelLec ligand(s) were detected by ELISA primarily in the alkali insoluble fraction of the *A. fumigatus* conidial cell wall whose primary constituents are carbohydrates (β-glucan, chitin and galactomannan) and melanin7 (Fig. 2a). Using the Fc-MelLec fusion protein as a probe to screen a neoglycolipid-based glycan microarray containing almost 500 structures, including oligosaccharides derived from glucans and chitin that are found in fungi8 (Supplementary Table 1), did not reveal any carbohydrate ligands for MelLec, unlike the C-type lectin Langerin, which was used as a control (Extended data Fig. 2). We then used Fc-MelLec to screen *A. fumigatus* conidia that were mutated in a variety of relevant cell-wall biosynthetic pathways by flow cytometry and immunofluorescence microscopy. Using this approach, we found that the ability of Fc-MelLec to detect conidia was lost specifically in the Δ*pksP* mutant, which is deficient in the ability to synthesise heptaketide naphthopyrone (YWA1), the first intermediate of the DHN-melanin biosynthetic pathway2,9 (Fig. 2b and Extended data Fig. 3a). We could also confirm loss of the MelLec ligand on Δ*rodA*Δ*pksP* double mutant conidia10, lacking both melanin and the hydrophobin layer, using flow cytometry, immunofluorescence microscopy and our MelLec reporter cells (Extended data Fig. 1f and 3b,c). Loss of *pksP* did not affect conidial recognition by Fc-Dectin-1 (Extended data Fig. 3c,d). Moreover, we could demonstrate a direct interaction of MelLec with *A. fumigatus* melanin ghosts (Extended data Fig. 3e). MelLec specifically recognised DHN-melanin, since this receptor did not detect melanin synthesised via other pathways, such as the L-Dopa pathway that is present in *Cryptococcus neoformans,* and in mammalian B16 melanoma cells11 (Extended data Fig. 3f). In addition to *A. fumigatus*, we could show that MelLec recognised other pigmented fungi that produced DHN-melanin, including *F. pedrosoi* and *C. cladosporioides*12 (Fig. 1b and Extended data Fig. 1e).

Although its tertiary structure is unresolved11, the biosynthetic pathway of DHN-melanin is well characterised in *A. fumigatus*3. To determine at which stage MelLec ligand(s) were being synthesised in the pathway, we screened mutants of *A. fumigatus* that were deficient in the enzymes catalysing each step, using Fc-MelLec and immunofluorescence microscopy, or ELISA. We confirmed that MelLec recognition was lost in Δ*pksP* conidia, however, MelLec recognition was unaffected in mutants deficient in all other stages of the DHN-melanin biosynthetic pathway (Fig. 2c and Extended data Fig. 4a). Using a pre-adsorption assay, we could show that recognition of wild-type conidia could be inhibited by pre-treating Fc-MelLec with Δ*ayg1* ghosts (defective in the second biosynthetic step, where MelLec ligands are still present), but not ghosts of Δ*pksP* (the first biosynthetic step, which lack MelLec ligands; Extended data Fig. 4b). We purified heptaketide naphthopyrone (YWA1) from Δ*ayg1* conidia13 and demonstrated that pre-treatment with this compound inhibited the

ability of Fc-MelLec, but not Fc-Dectin-1, to detect Δ*rodA* or NaOH-treated wild-type conidia (Extended data Fig. 4c-d). Moreover, we could demonstrate a direct interaction of MelLec with purified YWA1 (Fig. 2d) by ELISA. This suggested that the ability of MelLec to recognise this compound, as well as all the other melanin biosynthetic intermediates (Fig. 2c), was through recognition of the conserved naphthalene-diol unit, present in each of the intermediates. Indeed, we were able to show direct interaction of MelLec with 1,8-dihydronaphthalene (1,8-DHN), another upstream intermediate of the melanin biosynthetic pathway, by ELISA (Extended data Fig. 4e). Moreover, the structural isomers 1,2-DHN and 1,4-DHN, which contain the naphthalene-diol unit but are not melanin intermediates, were also recognised by MelLec (Extended data Fig. 4f). This suggests that the position of at least one of the hydroxyls (on carbon 2, 4 or 8) on the naphthalene-diol unit is not important for MelLec recognition. In contrast, naphthalene and 1-naphthol were not recognised by MelLec (Extended data Fig. 4g), indicating that the ligand of MelLec is a naphthalene-diol.

CLRs involved in fungal recognition are predominantly expressed by myeloid cells and are detectable in most tissues1. By RT-PCR, MelLec was widely expressed in mice, with the highest levels of transcript detected in the lung (Extended data Fig. 5a). To explore expression at a cellular level, we generated monoclonal antibodies (mAbs) by immunising rats with murine Fc-MelLec and then screening ELISA positive hybridoma supernatants by flow cytometry on NIH3T3 cells transfected to express full length HA-tagged murine MelLec. In these transfected cells, we found MelLec to be expressed as a glycosylated monomer at the cell surface, demonstrating that this CLR did not require an adaptor for surface expression1,14 (Extended data Fig. 5b,c). Although able to sense melanin (Fig. 2 and Extended data Fig. 1f), expression of MelLec did not confer the ability to capture *A. fumigatus* conidia to the cell surface of the transfected NIH3T3 cells (Extended data Fig. 5d).

Two mAbs (18E4 and 14C8) specific for MelLec were chosen for further characterisation of receptor expression on murine cells and tissues (Extended data Fig. 5e). Surprisingly, MelLec was not expressed by any murine myeloid cell population examined (either *ex-vivo* or *in vitro* bone marrow-derived), even following microbial stimulation, nor was this receptor expressed by cells in peripheral blood, bone marrow, lymphoid tissues or on platelets15 (Extended data Fig. 6a-c). Given the abundance of transcript, we next examined disaggregated lung tissue by flow cytometry which revealed a distinct population of cells that expressed MelLec (Fig. 3a). Histological visualisation of MelLec expression by immunofluorescence microscopy revealed broad punctate expression of this receptor throughout the lung tissue (Fig. 3b and Extended data Fig. 7m). A similar punctate staining pattern was also observed in the MelLec-expressing transfected NIH3T3 fibroblasts (Extended data Fig. 7a). By flow cytometry, we could show that MelLec expression was restricted to non-hematopoietic ($CD45^-$) cells (Fig. 3c and Extended data Fig. 7b). Further characterisation of these cells revealed that MelLec was expressed by $CD31^+$ $EpCAM^-$ endothelial cells (Fig. 3d). Expression of MelLec was also detected on $CD31^+$ endothelial cells in all other tissues tested, including the liver, heart, kidney and small intestine (Extended data Fig. 7c-f). However, we also detected a unique population of $CD31^+$ cells which co-expressed $EpCAM^+$, but only in the lung and liver, and these cells also expressed

MelLec (Fig. 3d and Extended data Fig. 7c). MelLec was not expressed on EpCAM$^+$ cells in other tissues, including the epidermis (Extended data Fig. 7g-j).

To gain insight into the physiological functions of MelLec, we generated mice deficient in this receptor using a conventional gene-targeting vector (Extended data Fig. 7k,l). Exons 1–5 of the gene encoding MelLec (*CLEC1A*) were deleted, which correspond to the cytoplasmic tail, transmembrane, stalk and part of the CRD region. Flow cytometry of disaggregated lung tissue, and immunofluorescence microscopy of whole lung, confirmed the lack of MelLec expression in cells from knockout mice (Fig. 3b and Extended data Fig. 7m,n). The MelLec-knockout mice were viable, had no gross abnormalities and had normal peripheral leucocyte counts (Supplementary Table 2). Intratracheal (i.t.) challenge of immunocompetent MelLec-knockout mice with wild type *A. fumigatus* conidia revealed no alterations in survival or other physiological parameters, including weight (Extended data Fig. 8a). However, a significantly reduced influx of neutrophils into the lungs of MelLec-knockout mice could be detected shortly (4 h) after i.t. challenge (Extended data Fig. 8b-d), before the conidia had germinated16. This alteration in cellular recruitment in the MelLec-knockout mice was associated with alterations in selected neutrophil-related cytokines, including KC and GM-CSF (Extended data Fig. 8e). Similar alteration in neutrophil recruitment was also observed in the MelLec-knockout mice following i.t. challenge with melanin ghosts of *A. fumigatus* (Extended data Fig. 8f). There were no alterations in other pulmonary myeloid populations following conidial challenge and by 24 h post challenge the difference in neutrophil influx was no longer apparent (Extended data Fig. 8g-h). There were also no changes in expression of MelLec during infection with *A. fumigatus* (Extended data Fig. 8i). Notably, the early neutrophil recruitment defect in the MelLec-knockout mice was lost upon i.t. challenge with Δ*pksP* conidia, which lack melanin (Extended data Fig. 8j,k).

We next examined the role of MelLec during infections in corticosteroid-treated mice, to model the effects of immunosuppression17. Under these conditions, loss of MelLec did not significantly alter susceptibility to infection (Extended data Fig. 9a). However, when we intravenously (i.v.) infected immunocompetent MelLec-knockout mice with *A. fumigatus* conidia17, we observed substantially increased susceptibility in these mice compared to wild-type animals (Fig. 4a). This increased susceptibility was associated with increased fungal burdens in several tissues, including the brain (Fig. 4b and Extended data Fig. 9b-d), as well as alterations in inflammatory responses (Fig. 4c). IL-17 responses were unaffected18. Consistent with a role in melanin recognition, there was no difference in susceptibility or fungal burdens between wild-type and MelLec-knockout mice following systemic infection with Δ*pksP* conidia (Fig. 4d and Extended data Fig. 9e).

Our murine data suggested that MelLec plays a key role in immunity to disseminated infections with *Aspergillus.* Therefore, we next explored the role of this receptor in humans. In humans, MelLec has previously been detected on endothelial cells19,20 but also myeloid cells5,18–20, and we could demonstrate that a human MelLec Fc fusion protein (Fc-hMelLec) recognises DHN-melanised conidia (Extended data Fig. 10a). A common missense single nucleotide polymorphism (SNP) within the coding region of *CLEC1A* (rs2306894, global MAF=0.3295) results in an amino acid change (Gly26Ala) in the cytoplasmic tail of hMelLec. Strikingly, we found a highly significant association between

Europe PMC Funders Author Manuscripts

this SNP and the risk of aspergillosis in stem-cell transplant recipients (Fig. 4e). This increased risk occurred when the variant was carried by the donor, but not when carried by the recipient. This suggests that in humans, the protective functions of MelLec are primarily mediated by myeloid cells. In our mouse model, there was no difference in resistance to infection upon adoptive transfer of MelLec-deficient bone-marrow into irradiated wild-type recipients (Extended data Fig. 10b).

To demonstrate a functional effect of the SNP in MelLec on myeloid cell function, we analysed the responses of monocyte-derived macrophages isolated from healthy genotyped donors. We found that macrophages from the individuals carrying this SNP produced significantly less IL-1β and IL-8 following *in vitro* stimulation with *A. fumigatus* conidia compared to controls (Fig. 4f), whereas there was no difference in response upon stimulation with LPS (Extended data Fig. 10c). We verified the inflammatory defect caused by this SNP in PBMCs isolated from an independent cohort (Extended data Fig. 10d). Moreover, using transduced RAW264.7 macrophages, we could directly demonstrate that this SNP results in an inflammatory defect upon stimulation with melanin-containing conidia (Extended data Fig. 10e).

In summary, melanin is considered a fungal virulence factor, providing protection against reactive oxygen species and inhibiting host cell phagocytosis, cytokine production and apoptosis3,10,21. Here we show that fungal DHN-melanin is also sensed by the host, through a Melanin sensing C-type Lectin receptor (MelLec) that plays a crucial role in controlling systemic *A. fumigatus* infection in both mice and humans. However, the data presented here, as well as early studies in rats18,22, show that the cellular expression of this receptor differs between species. Critically, we define a polymorphism of this receptor that, when present in donor cells, increases the susceptibility of stem-cell transplant recipients to disseminated aspergillosis. Our data therefore suggest that identifying donors carrying this SNP could significantly help reduce the incidence of this disease in transplant recipients. It is likely that MelLec will have an important role in immunity to other melanised fungi and black yeasts23, especially those that cause phaeohyphomycosis, mycetoma, and chromoblastomycosis.

Methods

Mice and fungal strains

C57BL/6 and MelLec$^{-/-}$ mice (8-12 weeks old) were obtained from the specific pathogen-free facility at the University of Aberdeen. Animal experiments were performed using age-matched female mice and conformed to the animal care and welfare protocols approved by UK Home Office (project license 70/8073) in compliance with all relevant local ethical regulations. MelLec$^{-/-}$ mice were generated commercially (TaconicArtemis) by conventional gene targeting in C57BL/6 embryonic stem cells as detailed in Extended data Fig. 7. Mice were randomly assigned to experimental or control groups, co-housed, and experiments were not blinded.

A. fumigatus isolate 13073 (American Type Culture Collection) and a clinical isolate CBS 144-8924 were used as wild-type strains. Melanin mutant strains (Δ*alb1*(*pksP1*), Δ*ayg1*,

Δ*abr1*, Δ*abr2*, Δ*arp1* and Δ*arp2* in the B5233 wild-type background) were generated previously25. Δ*rodA* and Δ*pksP*Δ*rodA* deletion mutants were generated as described9,10,24. Wild-type CBS110.4626 and CBS386.7526 strains with white conidia were also used, as indicated. All strains were maintained on 2% (w/v) malt-agar slants or potato dextrose agar in culture flasks; conidia were harvested and washed before use. Swollen/germinating morphotypes were obtained upon incubating conidia in Sabouraud liquid culture medium at 37°C for different time intervals, as indicated.

Fc-MelLec production and immunolabelling

Soluble chimeric proteins containing the stalk and CTLD of murine and human MelLec fused to the mutated Fc portion of human IgG1 were generated essentially as described previously27. Briefly, the relevant portions of the MelLec encoding genes were amplified by PCR (mouse primers, GAATTCCTCGAGCTGGAGCTCTCCAGGTAC and AAGCTTTCTACCAGCTGTCTAAT; human primers; GGGATCCACTACTACCAGCTCTCC and TGGATATCTGTCACCTTCGCCTAATGTTTC), and cloned into the pSecTag2 expression vector (Invitrogen Life Technologies) containing the mutated form of human IgG128. Sequenced constructs were transfected into HEK293T cells using Fugene 6 (Promega), as per manufacturer's instructions. Fusion proteins were purified from conditioned supernatants by chromatography on protein A Sepharose and dialysed against PBS. Fc-Dectin-127 and Fc-CLEC12b29 were generated similarly and used as controls.

For flow cytometry, fungi were incubated in 1-3% (w/v) BSA in PBS and Fc-proteins were added to a final concentration of 5 μg/mL. Following incubation at 4°C, fungal particles were washed in FACS buffer (0.5% (w/v) BSA and 2 mM EDTA in PBS), and bound Fc-proteins detected with allophycocyanin (APC) or phycoerythrin (PE)-conjugated donkey anti-human antibody (Jackson ImmunoResearch), fixed in 1% (v/v) formaldehyde, and analysed.

For microscopy, para-formaldehyde fixed conidia were taken for immunolabelling6. To obtain NaOH treated conidia, 1 M NaOH was added to conidia and heated in a boiling water bath for 1 h, followed by centrifugation to collect conidia and extensive washing. Melanin ghosts were isolated from conidia (B5233 as well as melanin mutant strains) by harsh chemical treatments that degrade other cellular components and result in hollow spherical-shaped melanin shells ("melanin ghosts"), as described before30. For immunostaining, fungal particles were incubated with 5 μg/mL Fc-MelLec in PBS containing 1% (w/v) BSA for 1 h. Following washing, bound Fc-MelLec was detected with fluorescein isothiocyanate (FITC)-labelled goat anti-human Fc-specific IgG (Sigma) in PBS containing 1% (w/v) BSA and washed with PBS-Tween. Conidia incubated with FITC-labelled anti-human Fc-specific IgG only were used as a negative control (data not shown). Labelled conidia were observed by fluorescence microscopy (Leica DMLB, USA).

In some experiments, Fc-proteins were pre-treated with either ghosts of melanin mutant strains, as indicated, or heptaketide naphthopyrone (YWA1), which was isolated from *AYG1* deletion mutant conidia as described previously13.

Monoclonal antibody production

The generation of monoclonal antibodies (mAb) to MelLec was performed essentially as described previously31. In brief, Sprague Dawley rats were immunised with Fc-MelLec in Freund's complete adjuvant. After a final intraperitoneal boost, without adjuvant, rat splenocytes were harvested and fused with Y3 myeloma cells, as described32. Hybridoma supernatants were screened by ELISA and positives were then tested by immunohistochemistry and flow cytometry, as described below, against Fc-MelLec as well as MelLec transduced NIH3T3 fibroblasts. Two mAbs (14C8 and 18E4; both IgG1) were selected for further use. Where required, mAbs were biotinylated with Sulfo-NHS-LC Biotin (Pierce), as described by the manufacturer.

Cell culture and growth conditions

Cells were maintained at 37°C and 5% CO_2 in DMEM or RPMI medium supplemented with 10% heat-inactivated foetal calf serum, 100 units/mL penicillin, 0.1 mg/mL streptomycin, and 2 mM L-glutamine. Phoenix ecotropic packaging cells (Plat-E) were maintained with the addition of 1 μg/mL puromycin and 10 μg/mL blasticidin (Life Technologies, Inc.).

NIH3T3 fibroblasts stably expressing full length murine or human MelLec were generated essentially as described for Dectin-133. Briefly, hemagglutinin (HA)-tagged MelLec was generated through PCR amplification (mouse primers, GGATCCACCATGCAGGCCAAATACAGCA and CTCGAGCTACTGGAGCTCTCCAGGTAC; human primers, AAAGGATCCACCATGCAGGCCAAGTACAGCAGCAC and AGCGTAATCCGGAACATCGTATGGGTACTCGAG) and subcloning into pFb-neo (Stratagene). Constructs were transfected into Plat-E retroviral packaging cell lines using Fugene 6 and retrovirus containing supernatants were used to transduce NIH3T3 fibroblasts in the presence of polybrene (Sigma). Stably transfected cells were selected using 600 μg/mL G418 (ThermoFisher Inc.). The expression of the receptor was confirmed by flow cytometry and Western Blotting, using the anti-HA antibody (Covance). In some experiments, NIH3T3 cells expressing murine CLEC12A31 were used as controls.

ELISA assays

Alkali-insoluble and soluble fungal cell wall fractions were obtained as described previously34. For the ELISA, wells were coated overnight with 20-200 μg/mL of the cell wall fractions, melanin ghosts (in house generated), purified YWA1 (in house generated), 1,8-DHN, 1,2-DHN, 1,4-DHN, naphthalene, 1-naphthol (all from Sigma) in 50 mM carbonate buffer pH 9.6, and then blocked with 1% BSA in PBS. Fc-MelLec (5 μg/mL) was added to the wells and incubated for 1 h at room temperature. Following washing with PBS-Tween-20 (0.5% (v/v)), peroxidase-conjugated human Fc-specific IgG (Sigma) was added to the wells and incubated for 1 h at room temperature. Following further washing, quantification of Fc-MelLec binding was detected using ortho-phenylenediamine (OPD, Sigma) and H_2O_2 detection system (Merck). The reaction was stopped using 4% (v/v) H_2SO_4 and optical densities measured at 492 nm.

Europe PMC Funders Author Manuscripts

Expression analysis

Peripheral blood leucocytes, resident and thioglycolate-elicited inflammatory peritoneal cells, alveolar macrophages and bone marrow cells were isolated essentially as described previously35. For platelets, peripheral blood was collected in 3.8% (w/v) sodium citrate buffer and centrifuged at 200*x*g at 25°C. The supernatant, containing platelet rich plasma, was used for subsequent analysis. Bone marrow-derived macrophages or dendritic cells, generated using L929 conditioned medium or 20 ng/mL GM-CSF (R&D Systems), respectively, were prepared as described31. In some experiments, cells were stimulated with 100 ng/mL lipopolysaccharide from *Escherichia coli* (Sigma).

Tissues isolated from mice were cut into small pieces and incubated for 30 min at 37°C with Liberase (Roche) and DNAse (Roche) in RPMI (Gibco), except for the small intestine which was incubated with Collagenase VIII (Sigma-Aldrich). Cells were disaggregated using the gentleMACS™ Dissociator (Miltenyi), strained through 70 μm nylon cell strainers (Fisher Scientific) and collected by centrifugation. Red blood cells were removed using Pharm Lyse (BD Biosciences).

For flow cytometry, isolated cells were washed in FACS wash (PBS with 0.5% (w/v) BSA and 5-10 mM EDTA) containing anti-CD16/CD32 (Clone 2.4G2, prepared in house). The following antibodies (all from BD Biosciences, eBioscience or Abcam) were used for FACS analysis of cell surface antigen expression following standard methodology: anti-MelLec-Biotin (described above), Streptavidin-PE-CF594 or Streptavidin-APC, anti-CD45.2-FITC (Clone 104), biotinylated anti-CD61 (clone 2C9.G2), anti-CD326-APC (EpCAM; Clone G8.8), anti-CD31-PE-Cyanine7 (PECAM-1; Clone 390), anti-Ly6G-APC (clone 1A8), anti-CD11b-PE-Cy7 (clone M1/70), CD11c-PerCP-Cy5.5 (clone HL3), anti-Siglec-F-BV421 (clone E50-2440), anti-CD45-PE-Cy7 (clone 30-F11), anti-CD11b-PerCP-Cy5.5 (clone M1/70), anti-CD11c-BV421 (clone HL3), anti-Siglec-F-PE (clone E50-2440) and anti-F4/80-AF700 (clone CL:A3-1) and isotype control AFRC MAC 49 (ECACC 85060404; isotype for anti-MelLec). Cell viability was detected using the fixable viability dye eFluor-780 (eBioscience) in PBS, and the cells were fixed with 1% formaldehyde prior to acquisition on a LSRII, LSR Fortessa or FACS Calibur (Becton Dickinson). Data were analysed using FlowJo. All contour plots are made using 2% probability contouring with outliers.

For immunofluorescence microscopy 6 μm alcohol fixed frozen lung sections were treated with Liberase (Roche) for 4 min at room temperature. Sections were blocked with 2% (v/v) normal goat serum, and incubated with anti-MelLec or isotype control for 1 h followed by Alexa Fluor 488 goat anti-rat (Invitrogen) for 30 min. Vectashield with DAPI or PI (Vector Laboratories Inc.) was used as a mountant for fluorescence, and slides were visualised using a Zeiss LSM 700 confocal microscope. Visualisation of transfected NIH3T3 cells was performed similarly, except the cells were fixed in 4% (v/v) paraformaldehyde prior to analysis.

Detection of MelLec in complementary DNA (cDNA) (Multiple Tissue Panels, Clontech) was performed using the Titanium Taq PCR kit (Clontech) with the following primers

CAGAGCCCAGGCACTCAGAGAATG and TGCGGGAGAGCCCTGTCCAAT. Expression of G3PDH was detected, as described previously36.

Murine infection models

For pulmonary infections, 10^5 (corticosteroid model) or 10^7 *A. fumigatus* ATCC 13073 conidia were administered to the caudal oropharynx of anesthetized mice. In some experiments, mice were administered with 0.6 mg of the corticosteroid, triamcinolone acetonide37 (Bristol-Myers Squibb), on days -1, 1 and 3, relative to infection on day 0. For systemic infections, 10^6 *A. fumigatus* ATCC 13073 conidia were administered to the lateral tail vein of mice. Mice were culled when they had lost 30% body weight or had become moribund. Pulmonary cellular inflammation was assessed by flow cytometry following total lung enzymatic digest, as described above, or in bronchoalveolar lavage (BAL) samples, isolated with PBS containing 5 mM EDTA (Gibco). Organs were homogenized in PBS and used for determination of fungal burdens and levels of inflammatory cytokines. Fungal burdens were determined by serial dilution onto potato dextrose agar plates and normalised to organ weights. Cytokines were measured by ELISA (R&D DuoSet), as described by the manufacturer, and normalized to protein concentration. Bone marrow chimeric mice were generated as described previously38.

Glycan microarray analyses

Microarray analyses were carried out using the neoglycolipid (NGL)-based microarray system 39. Details of the glycan probe library, the generation of the microarrays, imaging and data analysis are in the Supplementary Glycan Microarray Document (Supplementary Table 3) in accordance with the MIRAGE (Minimum Information Required for A Glycomics Experiment) guidelines for reporting glycan microarray-based data. The microarray contained 496 lipid-linked glycan probes (Supplementary Table 1). Microarray analysis of the soluble Fc-MelLec was performed essentially as described8. In brief, after blocking arrayed slides with 0.04% (v/v) Blocker Casein (Pierce), 1% (w/v) bovine serum albumin (Sigma A8577) in HEPES buffered saline (5 mM HEPES, pH 7.4, 150 mM NaCl, 5 mM $CaCl_2$), murine Fc-MelLec was precomplexed with biotinylated anti-human IgG (Vector) at a 1:3 ratio (w/w) before application onto the slides at a final concentration of 10 μg/mL. FLAG-tagged human Langerin was included as a positive control. The protein and rat anti-FLAG antibody mAb L5 were kindly provided by Chae Gyu Park (Yonsei University College of Medicine, Seoul). For analysis, the FLAG-tagged Langerin, was precomplexed with the rat anti-FLAG at a 1:3 ratio (w/w) and applied onto the slides at a final concentration of 5 μg/mL, followed by biotinylated anti-rat IgG (Pierce) (5 μg/mL). To detect binding Alexa Fluor-647-labeled streptavidin from Molecular Probes was used at 1 μg/mL. Data analysis and presentation was performed with dedicated glycan microarray software40.

Human studies

A total of 310 hematologic patients undergoing allogeneic hematopoietic stem cell transplantation at the Hospital of Santa Maria, Lisbon and Instituto Português de Oncologia (IPO), Porto, between 2009 and 2014 were enrolled in the study. The cases of invasive aspergillosis were identified and classified as “probable” or “proven” according to the

revised standard criteria from the European Organization for Research and Treatment of Cancer/Mycology Study Group (EORTC/MSG)41. Exclusion criteria included diagnosis of "possible" invasive aspergillosis, infection with invasive moulds other than *Aspergillus* spp. or history of pre-transplant mould infection. Study approval was obtained from the institutional review boards (SECVS-125/2014, HSM-632/14 and CES.26/015) and from the National Data Protection Commission (CNPD, 1950/2015) and was in compliance with all local relevant ethical regulations.

Genomic DNA was isolated from whole blood of recipients and donors (before transplantation) using the QIAcube automated system (Qiagen) at the regional centres of the Instituto Português do Sangue e Transplantação (Portugal). Genotyping of the nonsynonymous rs2306894 SNP in the *CLEC1A* gene was performed using KASPar assays (LGC Genomics) according to manufacturer's instructions in an Applied Biosystems 7500 Fast real–time PCR system (Thermo Fisher). Genotyping sets included randomly selected replicates of previously typed samples, and agreement between original and duplicate samples was ≥99%.

Peripheral blood mononuclear cells from healthy genotyped donors were enriched from buffy coats using Histopaque®-1077 (Sigma-Aldrich) and contaminating erythrocytes removed using Red Blood Cell Lysis Buffer (Sigma-Aldrich). Participants gave written informed consent prior to blood collection. Monocytes were isolated by positive selection using magnetically labelled $CD14^+$ MicroBeads (Miltenyi Biotec) on a MiniMACS separator and seeded at 10^6 cells/mL in 24-well plates for 7 days in RPMI-1640 medium supplemented with 10% (v/v) human serum and 20 ng/mL recombinant human granulocyte macrophage colony-stimulating factor (GM-CSF, Gibco). Acquisition of macrophage morphology was confirmed by phase contrast microscopy (Axiovert 135, Zeiss). For infection, macrophages were washed and then infected with live conidia of *A. fumigatus* strain A1163 at a ratio of 1:10 (cells/fungus) for 20 h at 37°C and 5% CO_2. Cytokines in supernatants were detected using DuoSet ELISA systems (BioLegend), according to the manufacturer's instructions. At least two technical replicates were performed for each donor.

For the independent cohort, genomic DNA was isolated from EDTA venous blood of healthy Dutch volunteers using the Gentra Pure Gene Blood kit (Qiagen, Venlo, The Netherlands) and genotyped for *CLEC1A* polymorphisms using the Illumina Immunochip SNP array platform, described previously42. Participants gave written informed consent prior to blood collection. As the *CLEC1A* SNP of interest (exonic rs2306894) was not represented on the genotyping platform, two intronic polymorphisms (rs7972187 and rs3825300) were used as markers. Linkage analysis revealed complete linkage disequilibrium of these two polymorphisms with the SNP of interest43 (R^2=1). 10^5 PBMCs isolated from genotyped donors were stimulated with 10^7 killed conidia/mL of the clinical isolate *A. fumigatus* V05-2744. After 24 h incubation in the presence of 10% human pooled serum at 37°C and 5% CO_2 supernatants were collected and IL-1β and IL-8 were measured by ELISA (R&D Systems, UK, and PeliKine, Sanquin, The Netherlands, respectively).

Europe PMC Funders Author Manuscripts

Statistical analysis

The probability of invasive aspergillosis resulting from *CLEC1A* rs2306894 SNP was analysed using the cumulative incidence method and compared using Gray's test45. Cumulative incidences were computed with the *cmprsk* package for R version 2.10.146, with censoring of data at the date of last follow–up visit and defining relapse and death as competing events. A period of 24 months after transplant was chosen to include all cases of fungal infection. Murine survival data were analysed with the log rank test using GraphPad Prism. No data was excluded.

In vitro and *ex-vivo* data were analysed using the GraphPad Prism software. Two-tailed student's t-tests or Mann-Whitney U tests were used to determine statistical significance. All experiments were independently repeated at least once, unless otherwise indicated. Sample sizes of at least five per group were chosen as this would allow the detection of a 25% difference in the mean between experimental and control groups with a probability of greater than 95% ($p < 0.05$), assuming a standard deviation of around 15% and a minimum power value of 0.8.

Europe PMC Funders Author Manuscripts

Extended Data

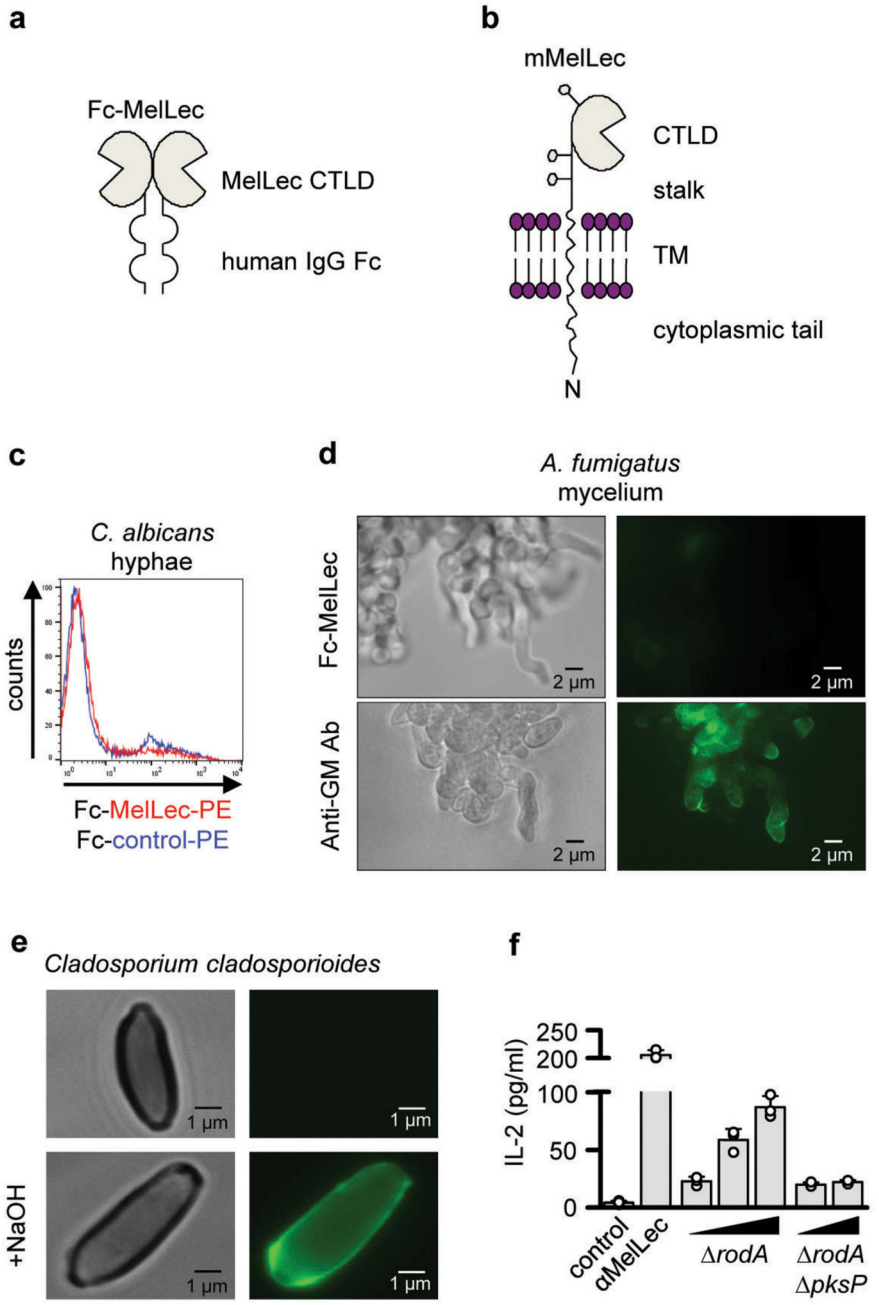

Extended data Figure 1. MelLec recognises ligands on selected fungi and fungal morphotypes.
Cartoon representation of the structure of Fc-MelLec (**a**) and the full length receptor (**b**). Lollipop structures represent predicted glycosylation sites. **c**, Fc-MelLec or Fc-CLEC12b (Fc-control) staining of *C. albicans* hyphae, generated in RPMI with 10% foetal bovine serum for 90 min. Fungal particles were analysed by flow cytometry. Experiment was repeated independently twice, with similar results. **d**, Representative light microscope

images and immunofluorescence micrographs using Fc-MelLec or anti-galactomannan (GM, control) as probes to detect ligands on *A. fumigatus* mycelium. **e**, Representative light microscope and immunofluorescence micrographs showing the surface distribution of MelLec ligands on *Cladosporium cladosporioides* using Fc-MelLec as a probe. Lower panels show fungal cells following treatment with 1M NaOH. **d-e** Experiments were repeated 3 times independently, with similar results. **f**, IL-2 production by MelLec-expressing BWZ reporter cells following stimulation by αMelLec antibody crosslinking or with Δ*rodA* (1:1, 5:1, 10:1) or Δ*rodA*Δ*pksP* (5:1, 10:1) *A. fumigatus* conidia, as indicated. Values shown are mean ± SD. Experiment was repeated 3 times independently, with similar results.

Europe PMC Funders Author Manuscripts

Europe PMC Funders Author Manuscripts

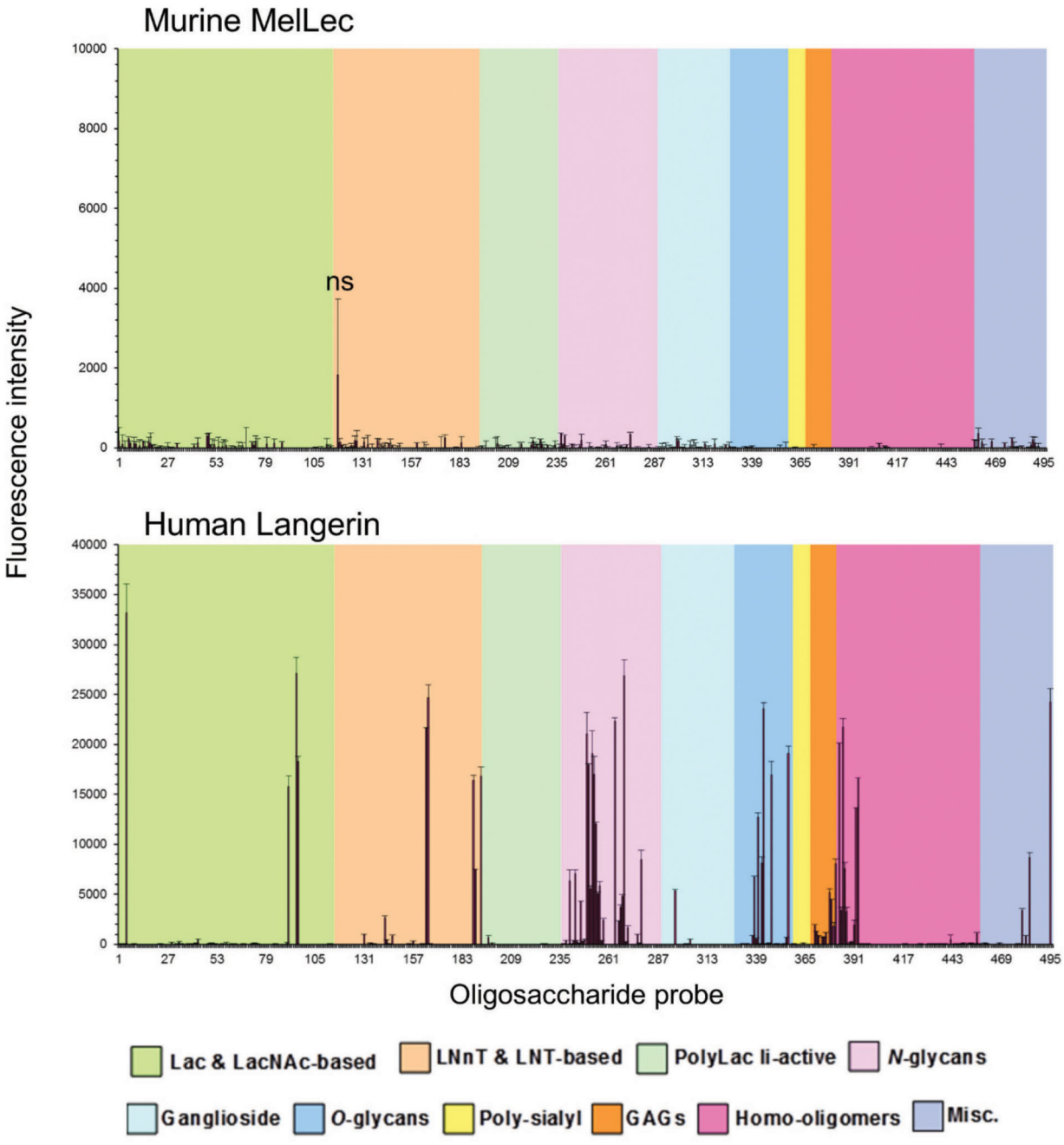

Extended data Figure 2. Glycan microarray analyses of murine Fc-MelLec and human Langerin.

These 496 lipid-linked probes are arranged according to their backbone sequences as annotated in the coloured panels below the figure. Lac, lactose; LacNAc, N-acetyllactosamine; LNnT, lacto-N-neotetraose; LNT, lacto-N-tetraose; PolyLac, polylactosamine; GAGs, glycosaminoglycans; Misc., miscellaneous. The signals are means of fluorescence intensities of duplicate spots, printed at 5 fmol per spot level with error bars representing half of the difference between the two values. The signals shown together with the probe sequences are in Supplementary Table 1. ns, not significant.

Europe PMC Funders Author Manuscripts

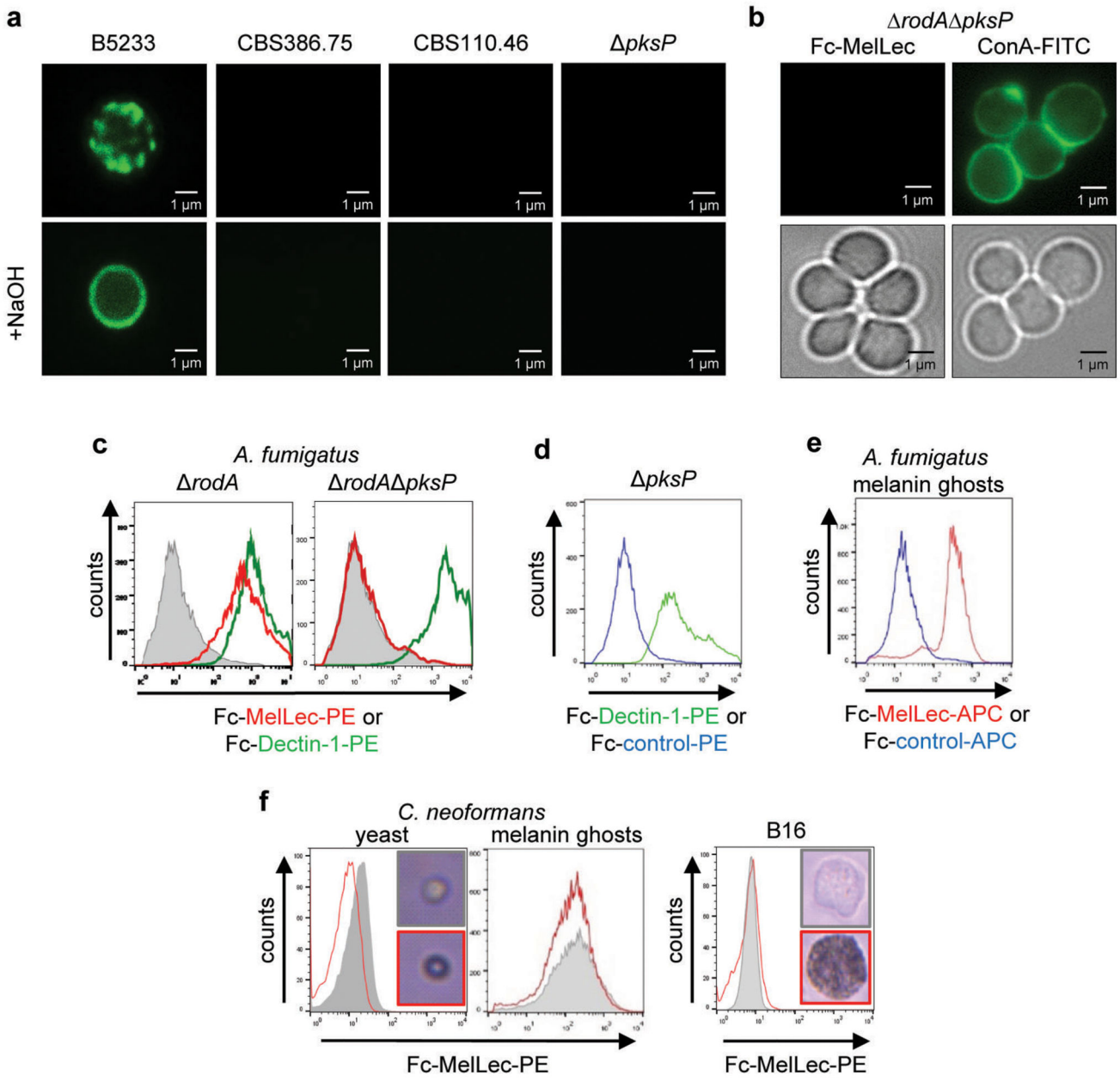

Extended data Figure 3. MelLec recognises DHN-melanin.

a, Representative immunofluorescence micrographs using Fc-MelLec as a probe showing the surface distribution of MelLec-ligands on *A. fumigatus* wild-type and a variety of melanin deficient mutants, as indicated. Lower panels show conidia treated with 1M NaOH. **b**, Representative immunofluorescence and light micrograph images of Δ*rodA*Δ*pksP A. fumigatus* conidia stained with Fc-MelLec or ConA-FITC, as indicated. **c**, Representative histograms showing the presence or absence of MelLec or Dectin-1 ligands on Δ*rodA* or Δ*rodA*Δ*pksP A. fumigatus* conidia, as indicated. Fungal particles were stained with Fc-MelLec (red) or Fc-Dectin-1 (green) and analysed by flow cytometry. Grey histograms indicate secondary only control. **d**, Representative histogram showing the presence Dectin-1

ligands on Δ*pksP A. fumigatus* conidia. Fungal particles were stained with Fc-Dectin-1 (green) or Fc-CLEC12b (Fc-control; blue) and analysed by flow cytometry. **e**, Representative histogram showing the presence MelLec ligands on melanin ghosts of *A. fumigatus* conidia. Fungal particles were stained with Fc-MelLec (red) or Fc-CLEC12b (Fc-control; blue) and analysed by flow cytometry. **a-e**, Experiments were repeated 3 times independently, with similar results. **f**, Flow cytometric analysis of melanised (red) and non-melanised (grey) *Cryptococcus neoformans* yeast and melanin ghosts, and B16 melanoma cells47, stained with Fc-MelLec, as indicated. Experiment was repeated independently twice, with similar results.

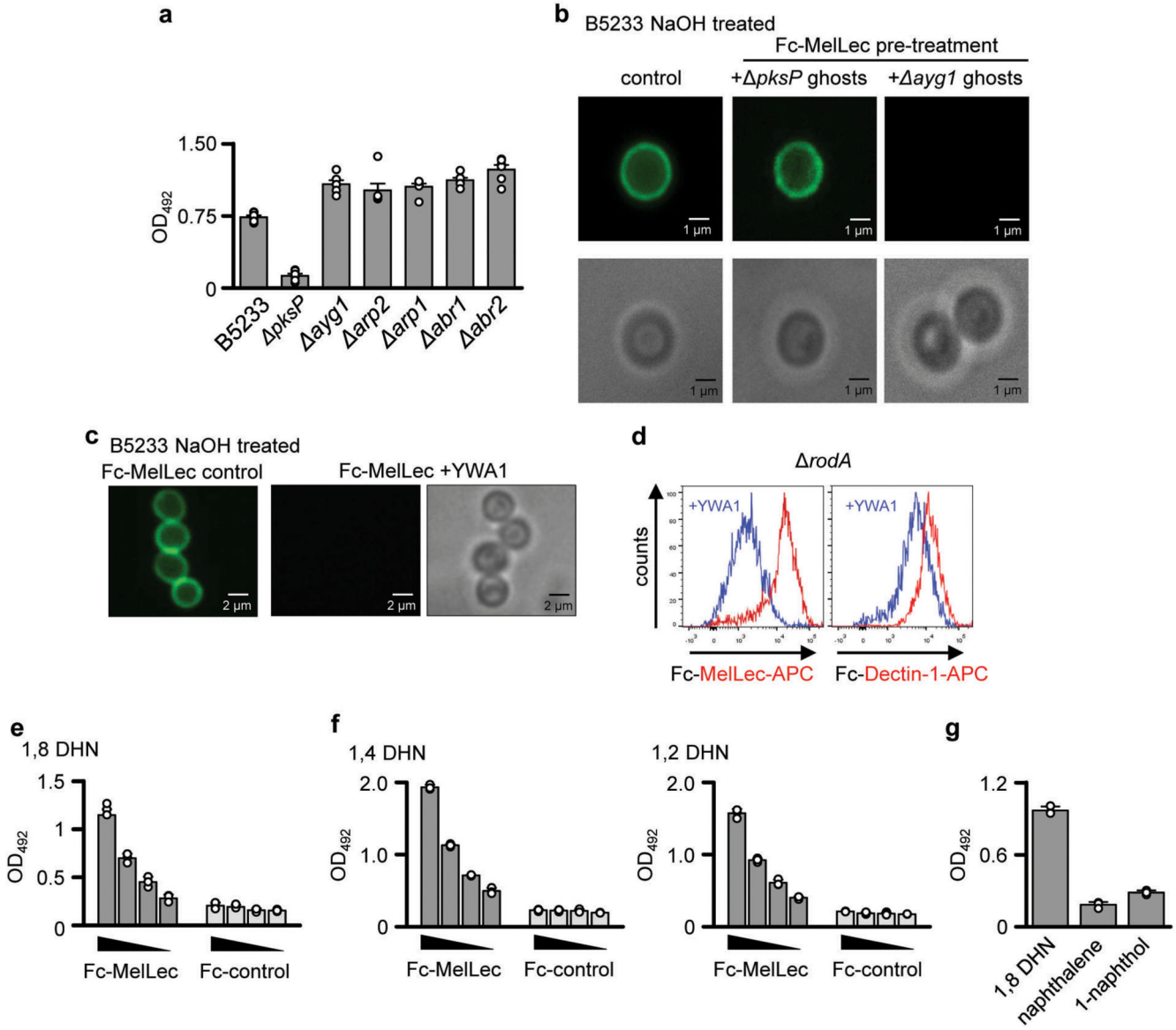

Extended data Figure 4. MelLec recognises naphthalene-diol.

a, Detection of MelLec ligands in ghosts of melanin mutants of *A. fumigatus* by ELISA, as indicated. Values show mean ± SD. **b**, Representative immunofluorescence and light

micrograph images of Fc-MelLec ligands on NaOH-treated *A. fumigatus* B5233 conidia following pre-treatment with ghosts of Δ*pksP* or Δ*ayg1* conidia, as indicated. **c**, Representative immunofluorescence and light micrograph images of MelLec ligands on NaOH-treated wild-type *A. fumigatus* conidia following pre-treatment with or without heptaketide naphthopyrone (YWA1). **a-c**, Experiments were repeated at least 3 times independently, with similar results. **d**, Detection of Fc-MelLec or Fc-Dectin-1 ligands on Δ*rodA* conidia following pre-treatment with (blue) or without (red) heptaketide naphthopyrone (YWA1). Experiment was repeated independently twice, with similar results. Detection of 1,8-DHN (**e**) and 1,2-DHN and 1,4-DHN (**f**) by Fc-MelLec and Fc-control using ELISA, as indicated. Values show mean ± SD. **g**, Detection of 1,8-DHN, naphthalene and 1-naphthol by Fc-MelLec using ELISA, as indicated. Values show mean ± SD. **e-g**, Experiments were repeated at least 3 times independently, with similar results.

Europe PMC Funders Author Manuscripts

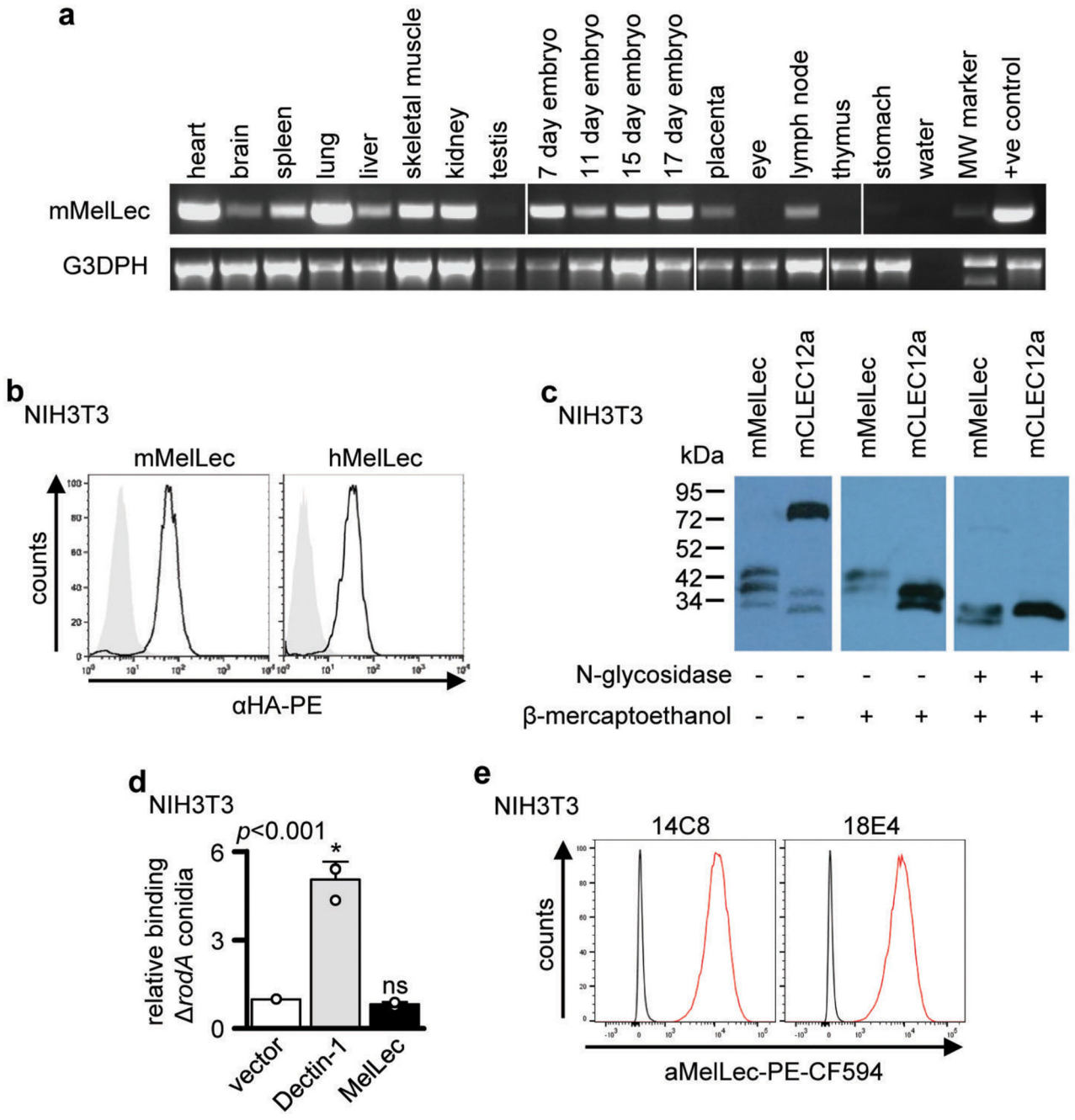

Extended data Figure 5. MelLec is expressed at the cell surface.

a, RT-PCR detection of MelLec expression in various tissues, as indicated. The expression of glycerol-3-phosphate dehydrogenase (G3PDH) in these samples, also used for the characterization of MCL36, is shown as a control. Experiment was performed once (for gel source data, see Supplementary Figure 1). **b**, Flow cytometric analysis of surface expression of HA-tagged murine and human MelLec on the surface of NIH3T3 fibroblasts (black open histograms). NIH3T3 cells transfected with vector only served as controls (grey filled histograms). **c**, Western blot analysis of lysates of HA-tagged mMelLec expressing NIH3T3

Europe PMC Funders Author Manuscripts

cells under reducing and non-reducing conditions and with and without N-glycosidase. HA-tagged mCLEC12A31 expressing NIH3T3 cells served as controls (for blot source data, see Supplementary Figure 1). **d**, Relative binding of FITC-labelled *ΔrodA A. fumigatus* conidia to NIH3T3 cells transduced with vector only, Dectin-1 or MelLec, as determined by flow cytometry. Values shown are mean ± SD, analysed by one-way ANOVA. **e**, Screening of hybridoma supernatants on mMelLec-expressing (red) and parental (black) NIH3T3 cells. **b-e**, Experiments were repeated at least 3 times independently, with similar results. *, p≤0.05; Ns, not significant.

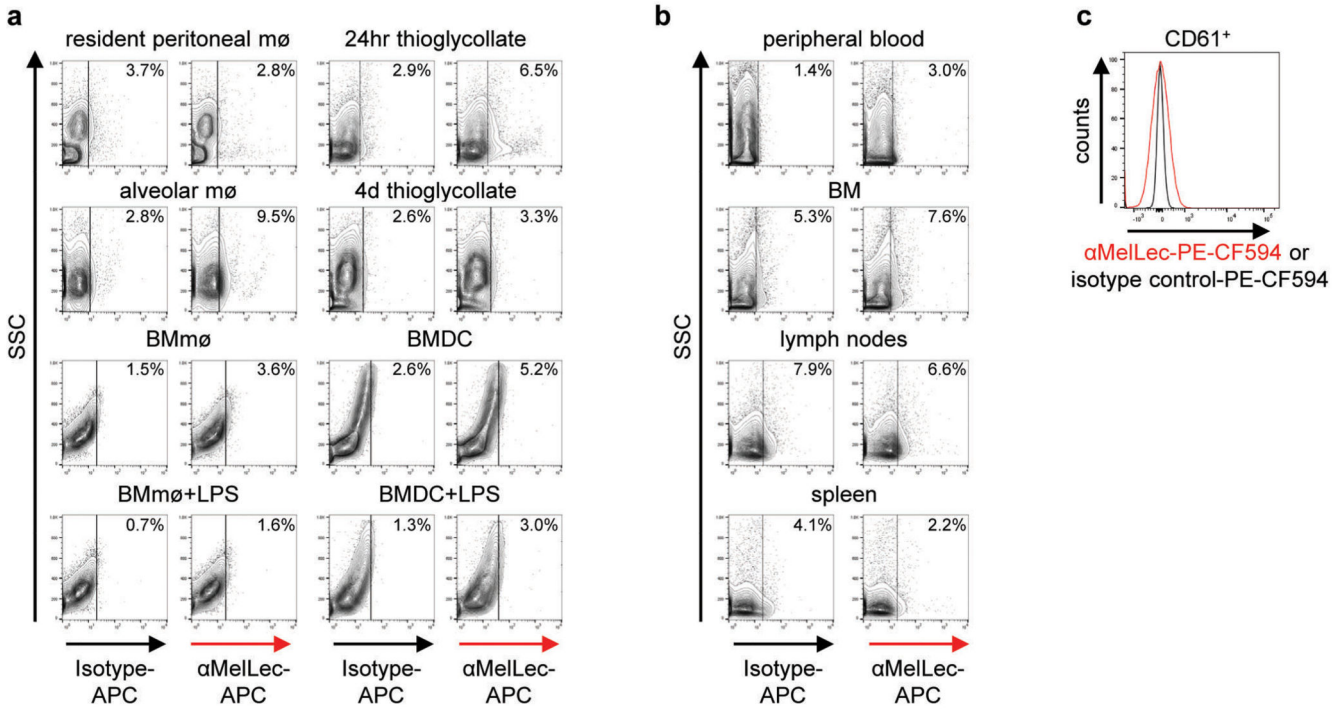

Extended data Figure 6. Murine MelLec is not expressed by myeloid cells.

Flow cytometric analysis of MelLec expression on various *ex vivo* and *in vitro* derived myeloid cells (**a**) and peripheral blood, bone marrow, lymph nodes and spleen (**b**), as indicated. **a-b**, Experiments were repeated at least twice independently, with similar results. **c**, Flow cytometric analysis of MelLec expression on $CD61^+$ platelets. Experiment was repeated at least 3 times independently, with similar results. BM, bone marrow; DC, dendritic cell; mø, macrophage; LPS, lipopolysaccharide.

Europe PMC Funders Author Manuscripts

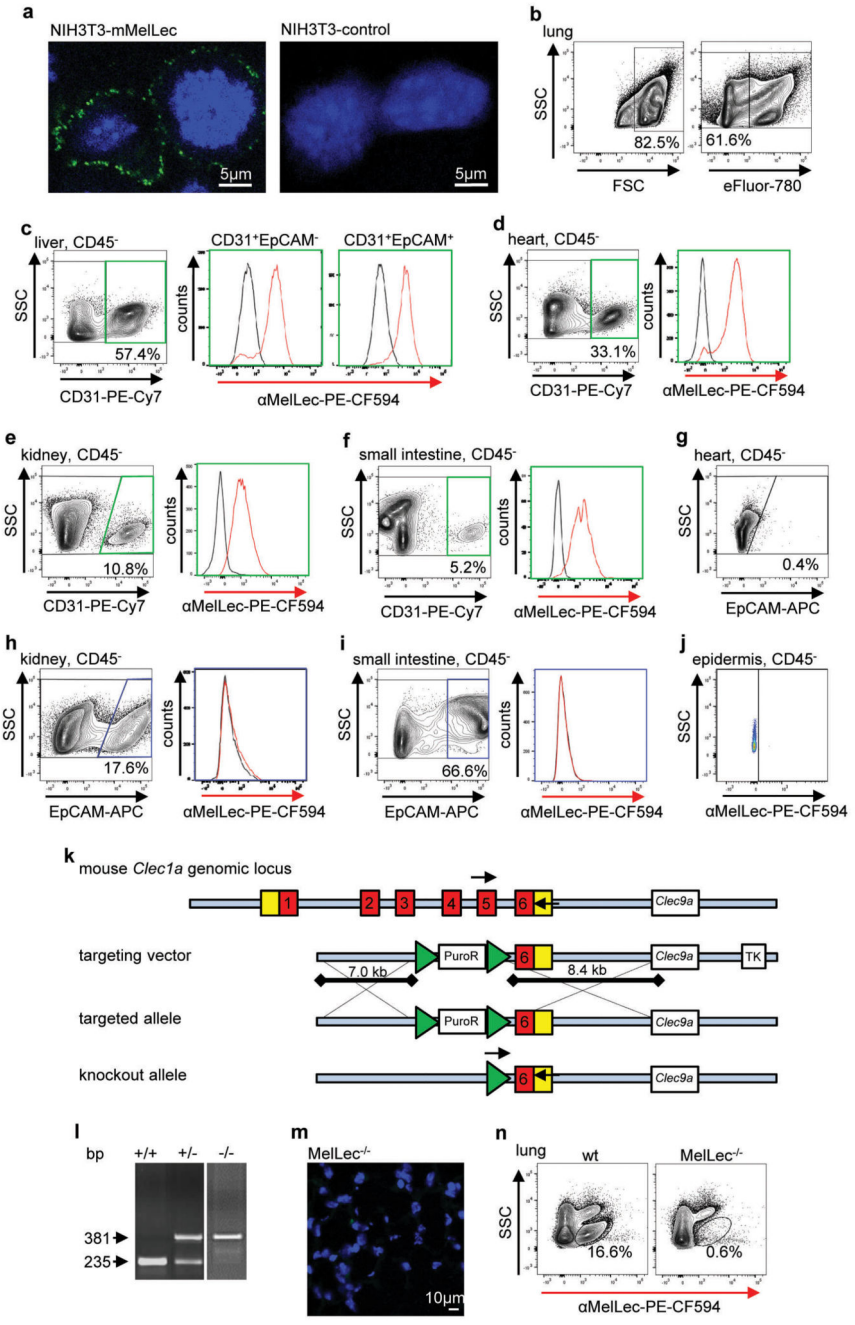

Extended data Figure 7. MelLec expression in tissues and generation of MelLec$^{-/-}$ mice.

a, Immunofluorescence microscopy of MelLec-expressing versus control NIH3T3 cells labelled with αMelLec (green). Nuclei are stained with DAPI (blue). Experiments were repeated at least 3 times independently, with similar results. **b**, Exemplar flow cytometric gating strategy for identification of live cells from tissue. **c**, Flow cytometric analysis of MelLec expression on live CD45$^-$ CD31$^+$ EpCAM$^-$ and EpCAM$^+$ populations in the liver, as indicated. Flow cytometric analysis of MelLec expression on live CD45$^-$ CD31$^+$ cells in the heart (**d**), kidney (**e**) and small intestine (**f**). Flow cytometric analysis of MelLec expression

on live CD45^{-}EpCAM^{+} cells in the heart (**g**), kidney (**h**), small intestine (**i**) and epidermis (**j**). **b-j** Experiments were repeated at least twice independently, with similar results. Black lines, isotype controls. **k**, Schematic representation of the wild-type *CLEC1A* locus, gene targeting vector, PCR primer sites, and correctly targeted recombinant gene-targeted allele. **l**, PCR analysis of gene-targeted mice (for gel source data, see Supplementary Figure 1). +/+, wild-type, +/- heterozygous and -/- homozygous for the targeted allele. **m**, Immunofluorescence microscopy of naïve lung tissue from MelLec$^{-/-}$ mice (labelling of wild-type lung is shown in Fig. 3b). **n**, Analysis of MelLec expression in disaggregated lung tissue from wild-type (wt) or MelLec$^{-/-}$ mice by flow cytometry. **l-n**, Experiments were repeated at least 3 times independently, with similar results.

Europe PMC Funders Author Manuscripts

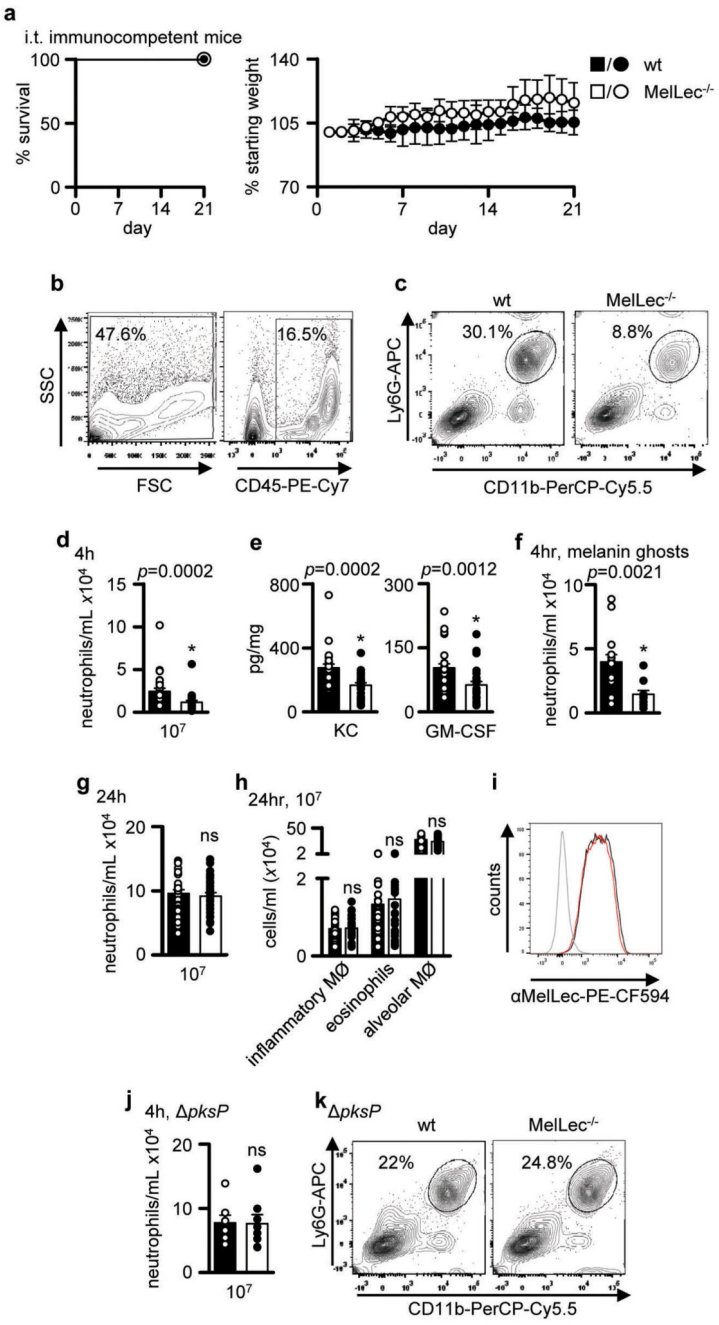

Extended data Figure 8. MelLec$^{-/-}$ mice show early inflammatory defects upon challenge with *A. fumigatus*.

a, Survival (left) and weight measurements (right) of immunocompetent mice following intratracheal (i.t.) infection with 10^7 *A. fumigatus* conidia (n=4 animals per group). Values shown are mean ± SD. **b**, Exemplar flow cytometric gating strategy for identification of CD45$^+$ cells from BAL. **c**, Representative FACS profiles of pulmonary CD11b$^+$ Ly6G^{high} neutrophils in wild-type and MelLec$^{-/-}$ mice 4 h after challenge with 10^7 *A. fumigatus* conidia (wt n=29 animals; MelLec$^{-/-}$ n=26 animals). Pulmonary CD11b$^+$ Ly6G^{high}

neutrophils (wt n=29 animals, MelLec$^{-/-}$ n=26 animals) (**d**) and cytokines (n=25 animals per group) (**e**) in mice 4 h after challenge with 10^7 *A. fumigatus* conidia, as indicated. **f**, Pulmonary CD11b$^+$ Ly6G^{high} neutrophils in mice 4 h after challenge with melanin ghosts (160 μg) of *A. fumigatus* (wt n=15 animals; MelLec$^{-/-}$ n=10 animals). Samples with blood contamination were excluded. **g**, Pulmonary CD11b$^+$ Ly6G^{high} neutrophils in mice 24 h after challenge with 10^7 *A. fumigatus* conidia (wt n=33 animals, MelLec$^{-/-}$ n=30 animals). **h**, Cellular inflammatory profiles of mice after 24 h challenge with 10^7 *A. fumigatus* conidia, as indicated (wt n=33 animals, MelLec$^{-/-}$ n=30 animals). Alveolar macrophages were defined as CD11c$^+$ Siglec-F$^+$, inflammatory macrophages as CD11b$^+$ F4/80$^+$ and eosinophils as CD11b$^+$ Siglec-F$^+$. **d-h**, Values shown are mean ± SEM of pooled data from at least two independent experiments, analysed by two-sided Mann-Whitney U test. **i**, Expression of MelLec on pulmonary CD45$^-$ CD31$^+$ cells isolated from uninfected mice (black) and mice 24 h after infection with *A. fumigatus* conidia (red). Grey line, isotype control (n=3 animals per group). **j**, Pulmonary CD11b$^+$ Ly6G^{high} neutrophils in mice 4 h after challenge with 10^7 Δ*pksP A. fumigatus* conidia (wt n=7 animals, MelLec$^{-/-}$ n=8 animals). Values shown are mean ± SEM of pooled data from two independent experiments, analysed by two-sided Mann-Whitney U test. **k**, Representative FACS profiles of pulmonary CD11b$^+$ Ly6G^{high} neutrophils in wild-type and MelLec$^{-/-}$ mice 4 h after challenge with 10^7 Δ*pksP A. fumigatus* conidia (wt n=7 animals, MelLec$^{-/-}$ n=8 animals). *, p≤0.05; ns, not significant.

Europe PMC Funders Author Manuscripts

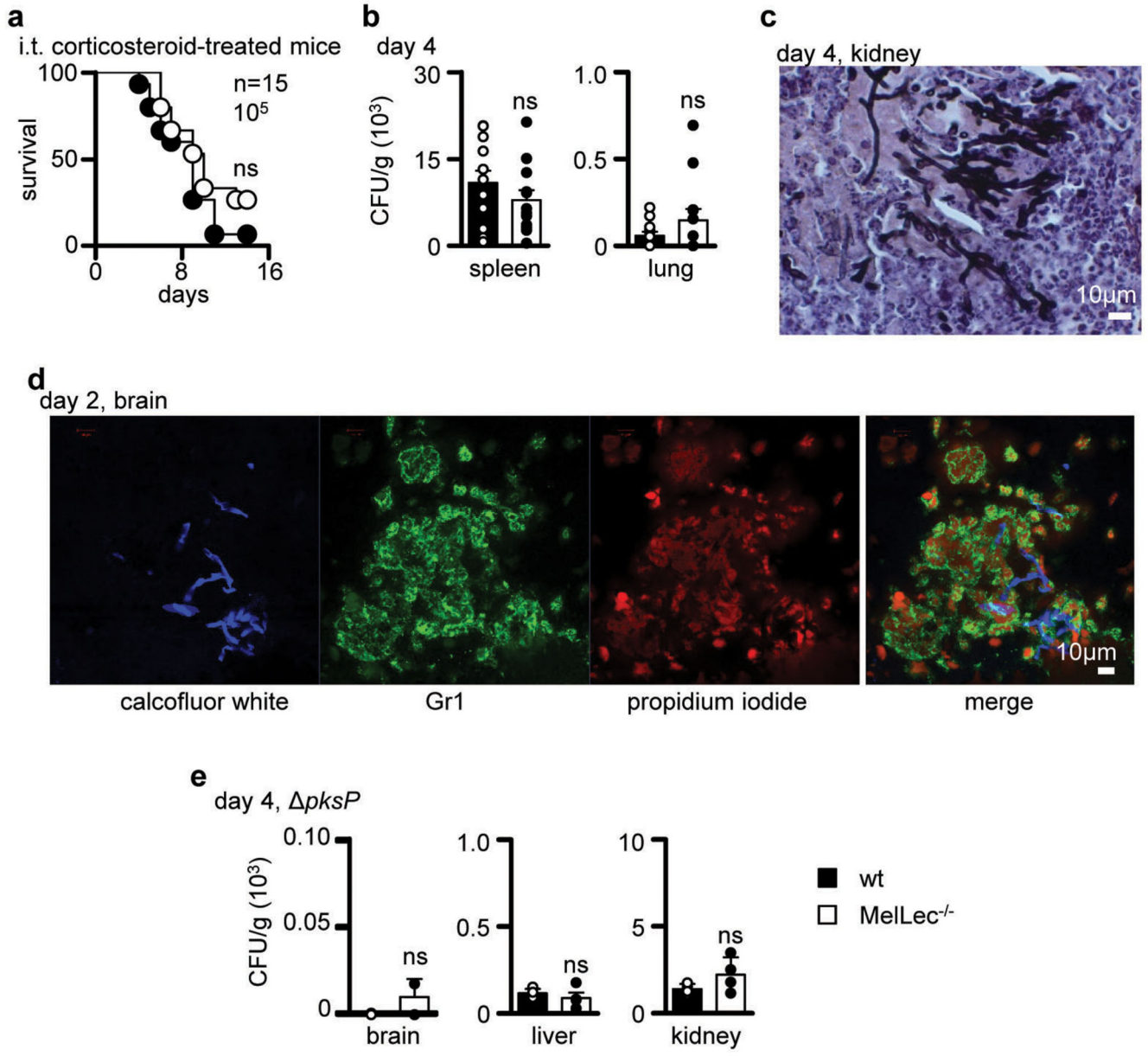

Extended data Figure 9. MelLec$^{-/-}$ mice show alterations in anti-fungal immunity during systemic infection.

a, Survival of corticosteroid treated mice following intratracheal (i.t.) infection with 10^5 *A. fumigatus* conidia (n=15 animals per group). Pooled data from two independent experiments, analysed by log-rank test. **b**, Fungal burdens in various mouse tissues, as indicated, 4 days after i.v. infection with 10^6 *A. fumigatus* conidia (n=12 animals per group). Values shown are mean ± SEM of pooled data from two independent experiments, analysed by two-sided Mann-Whitney U test. **c**, Tissue section of kidney from day 4 infected MelLec$^{-/-}$ mouse stained with Grocott's methenamine silver stain and haematoxylin (n=3 animals per group). **d**, Immunofluorescence microscopy of brain from day 2 infected MelLec$^{-/-}$ mouse (n=3 animals per group). Fungi are stained with calcofluor white (blue),

leukocytes with Gr1 (green), and DNA with propidium iodide (red). **e**, Fungal burdens in various mouse tissues, as indicated, 4 days after i.v. infection with 10^6 Δ*pksP A. fumigatus* conidia (n=4 animals per group). Values shown are mean ± SD, analysed by two-sided Mann-Whitney U test. *, p≤0.05; ns, not significant.

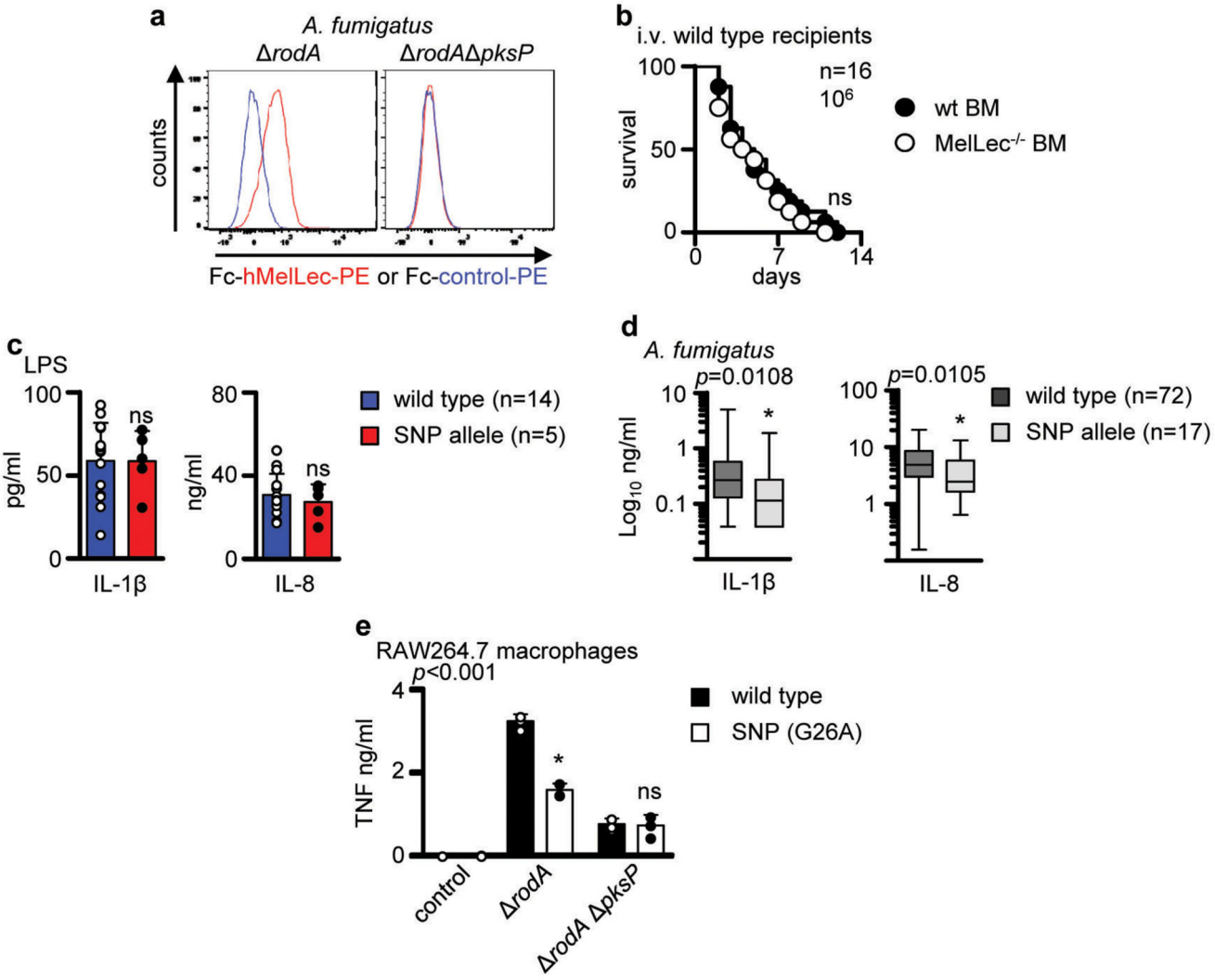

Extended data Figure 10. A SNP in human MelLec influences anti-*Aspergillus* inflammatory responses.

a, Representative histograms showing the presence or absence of human MelLec ligands on Δ*rodA* or Δ*rodA*Δ*pksP A. fumigatus* conidia, as determined by flow cytometry. Fc-CLEC12b was used as a control (Fc-control). Experiment was repeated at least 3 times independently, with similar results. **b**, Survival of irradiated wild-type mice reconstituted with wild-type or MelLec$^{-/-}$ bone-marrow (BM), as indicated, following i.v. infection with 10^6 *A. fumigatus* conidia (n=16 animals per group). Pooled data from two independent experiments, analysed by log-rank test. **c**, Inflammatory cytokine production in monocyte-derived macrophages isolated from genotyped individuals, following stimulation with LPS (wild-type n=14 individuals, SNP allele n=5 individuals). Values shown are mean ± SD,

Europe PMC Funders Author Manuscripts

analysed by two-sided Mann-Whitney U test. **d**, Inflammatory cytokine production in PBMCs isolated from genotyped Dutch individuals, following stimulation with heat-killed *A. fumigatus* conidia (wild-type n=72 individuals, SNP allele n=17 individuals). Boxes represent the median values and interquartile ranges; whiskers represent minimum and maximum values, analysed by two-sided Mann-Whitney U test. **e**, Inflammatory cytokine production in transduced RAW264.7 macrophages expressing wild-type or SNP allele following stimulation with Δ*rodA* or Δ*rodA*Δ*pksP A. fumigatus* conidia, as indicated. Values shown are mean ± SD, analysed by one-way ANOVA and repeated at least 3 times independently, with similar results. *, p≤0.05; ns, not significant.

Supplementary Material

Refer to Web version on PubMed Central for supplementary material.

Acknowledgements

We would like to thank the staff of the University of Aberdeen animal facility for their support and care for our animals, and Chae Gyu Park, Yonsei University College of Medicine, Seoul for providing recombinant Langerin. We thank Scott Filler and Robert Cramer for advice. Funding was provided by the Wellcome Trust (102705, 097377, 093378, 099197, 108430, 101873), the MRC Centre for Medical Mycology and the University of Aberdeen (MR/N006364/1). KJK is supported by the intramural program of the National Institute of Allergy and Infectious Diseases, National Institutes of Health, VA by ANR-DST COMASPIN grant (ANR-13-ISV3-0004), BH by German Science Foundation (www.dfg.de) grant no. HE 7565/1-1, JPL, IV and VA by the ANR and FRM DEQ2015-331722, AC by the Northern Portugal Regional Operational Programme (NORTE 2020), under the Portugal 2020 Partnership Agreement, through the European Regional Development Fund (FEDER) (NORTE-01-0145-FEDER-000013), and by the Fundação para a Ciência e Tecnologia (FCT) (IF/00735/2014 and SFRH/BPD/96176/2013).

References

1. Hardison SE, Brown GD. C-type lectin receptors orchestrate antifungal immunity. Nat Immunol. 2012; 13:817–822. [PubMed: 22910394]
2. Nosanchuk JD, Casadevall A. The contribution of melanin to microbial pathogenesis. Cell Microbiol. 2003; 5:203–223. [PubMed: 12675679]
3. Heinekamp T, et al. Aspergillus fumigatus melanins: interference with the host endocytosis pathway and impact on virulence. Front Microbiol. 2012; 3:440. [PubMed: 23346079]
4. Pyz E, Brown GD. Screening for ligands of C-type lectin-like receptors. Methods Mol Biol. 2011; 748:1–19. [PubMed: 21701963]
5. Colonna M, Samaridis J, Angman L. Molecular characterization of two novel C-type lectin-like receptors, one of which is selectively expressed in human dendritic cells. Eur J Immunol. 2000; 30:697–704. [PubMed: 10671229]
6. Aimanianda V, et al. Surface hydrophobin prevents immune recognition of airborne fungal spores. Nature. 2009; 460:1117–1121. [PubMed: 19713928]
7. Latge JP, Beauvais A. Functional duality of the cell wall. Curr Opin Microbiol. 2014; 20:111–117. [PubMed: 24937317]
8. Palma AS, et al. Ligands for the beta-glucan receptor, Dectin-1, assigned using "designer" microarrays of oligosaccharide probes (neoglycolipids) generated from glucan polysaccharides. J Biol Chem. 2006; 281:5771–5779. [PubMed: 16371356]
9. Jahn B, et al. Isolation and characterization of a pigmentless-conidium mutant of Aspergillus fumigatus with altered conidial surface and reduced virulence. Infect Immun. 1997; 65:5110–5117. [PubMed: 9393803]
10. Akoumianaki T, et al. Aspergillus Cell Wall Melanin Blocks LC3-Associated Phagocytosis to Promote Pathogenicity. Cell Host Microbe. 2016; 19:79–90. [PubMed: 26749442]

11. Nosanchuk JD, Stark RE, Casadevall A. Fungal Melanin: What do We Know About Structure? Front Microbiol. 2015; 6:1463. [PubMed: 26733993]
12. Llorente C, et al. Cladosporium cladosporioides LPSC 1088 produces the 1,8-dihydroxynaphthalene-melanin-like compound and carries a putative pks gene. Mycopathologia. 2012; 174:397–408. [PubMed: 22714980]
13. Tsai HF, et al. Pentaketide melanin biosynthesis in Aspergillus fumigatus requires chain-length shortening of a heptaketide precursor. J Biol Chem. 2001; 276:29292–29298. [PubMed: 11350964]
14. Sancho D, Reis e Sousa C. Signaling by myeloid C-type lectin receptors in immunity and homeostasis. Annu Rev Immunol. 2012; 30:491–529. [PubMed: 22224766]
15. Rambach G, et al. Identification of Aspergillus fumigatus Surface Components That Mediate Interaction of Conidia and Hyphae With Human Platelets. J Infect Dis. 2015; 212:1140–1149. [PubMed: 25810442]
16. Faro-Trindade I, et al. Characterisation of innate fungal recognition in the lung. PLoS ONE. 2012; 7:e35675. [PubMed: 22536422]
17. Clemons KV, Stevens DA. The contribution of animal models of aspergillosis to understanding pathogenesis, therapy and virulence. Med Mycol. 2005; 43(Suppl 1):S101–110. [PubMed: 16110800]
18. Lopez Robles MD, et al. Cell-surface C-type lectin-like receptor CLEC-1 dampens dendritic cell activation and downstream Th17 responses. Blood Advances. 2017; 1:557–568. [PubMed: 29296975]
19. Sobanov Y, et al. A novel cluster of lectin-like receptor genes expressed in monocytic, dendritic and endothelial cells maps close to the NK receptor genes in the human NK gene complex. Eur J Immunol. 2001; 31:3493–3503. [PubMed: 11745369]
20. Sattler S, et al. The human C-type lectin-like receptor CLEC-1 is upregulated by TGF-beta and primarily localized in the endoplasmic membrane compartment. Scand J Immunol. 2012; 75:282–292. [PubMed: 22117783]
21. Chai LY, et al. Aspergillus fumigatus conidial melanin modulates host cytokine response. Immunobiology. 2010; 215:915–920. [PubMed: 19939494]
22. Thebault P, et al. The C-type lectin-like receptor CLEC-1, expressed by myeloid cells and endothelial cells, is up-regulated by immunoregulatory mediators and moderates T cell activation. J Immunol. 2009; 183:3099–3108. [PubMed: 19667084]
23. Seyedmousavi S, et al. Black yeasts and their filamentous relatives: principles of pathogenesis and host defense. Clin Microbiol Rev. 2014; 27:527–542. [PubMed: 24982320]
24. Thau N, et al. Rodletless mutants of Aspergillus fumigatus. Infect Immun. 1994; 62:4380–4388. [PubMed: 7927699]
25. Tsai HF, Wheeler MH, Chang YC, Kwon-Chung KJ. A developmentally regulated gene cluster involved in conidial pigment biosynthesis in Aspergillus fumigatus. J Bacteriol. 1999; 181:6469–6477. [PubMed: 10515939]
26. Sarfati J, et al. A new experimental murine aspergillosis model to identify strains of Aspergillus fumigatus with reduced virulence. Nihon Ishinkin Gakkai Zasshi. 2002; 43:203–213. [PubMed: 12402022]
27. Graham LM, et al. Soluble Dectin-1 as a tool to detect beta-glucans. J Immunol Methods. 2006; 314:164–169. [PubMed: 16844139]
28. Ettinger R, Browning JL, Michie SA, van Ewijk W, McDevitt HO. Disrupted splenic architecture, but normal lymph node development in mice expressing a soluble lymphotoxin-beta receptor-IgG1 fusion protein. Proc Natl Acad Sci U S A. 1996; 93:13102–13107. [PubMed: 8917551]
29. Hoffmann SC, et al. Identification of CLEC12B, an inhibitory receptor on myeloid cells. J Biol Chem. 2007; 282:22370–22375. [PubMed: 17562706]
30. Bayry J, et al. Surface structure characterization of Aspergillus fumigatus conidia mutated in the melanin synthesis pathway and their human cellular immune response. Infect Immun. 2014; 82:3141–3153. [PubMed: 24818666]
31. Pyz E, et al. Characterisation of murine MICL (CLEC12A) and evidence for an endogenous ligand. Eur J Immunol. 2008; 38:1157–1163. [PubMed: 18350551]

32. Galfre G, Milstein C, Wright B. Rat x rat hybrid myelomas and a monoclonal anti-Fd portion of mouse IgG. Nature. 1979; 277:131–133. [PubMed: 310519]
33. Willment JA, Gordon S, Brown GD. Characterisation of the human {beta}-glucan receptor and its alternatively spliced isoforms. J Biol Chem. 2001; 276:43818–43823. [PubMed: 11567029]
34. Richie DL, et al. A role for the unfolded protein response (UPR) in virulence and antifungal susceptibility in Aspergillus fumigatus. PLoS Pathog. 2009; 5:e1000258. [PubMed: 19132084]
35. Taylor PR, Brown GD, Geldhof AB, Martinez-Pomares L, Gordon S. Pattern recognition receptors and differentiation antigens define murine myeloid cell heterogeneity ex vivo. Eur J Immunol. 2003; 33:2090–2097. [PubMed: 12884282]
36. Kerscher B, et al. Mycobacterial receptor, Clec4d (CLECSF8, MCL), is coregulated with Mincle and upregulated on mouse myeloid cells following microbial challenge. Eur J Immunol. 2016; 46:381–389. [PubMed: 26558717]
37. Shepardson KM, et al. Myeloid derived hypoxia inducible factor 1-alpha is required for protection against pulmonary Aspergillus fumigatus infection. PLoS Pathog. 2014; 10:e1004378. [PubMed: 25255025]
38. Redelinghuys P, et al. MICL controls inflammation in rheumatoid arthritis. Ann Rheum Dis. 2016; 75:1386–1391. [PubMed: 26275430]
39. Liu Y, et al. Neoglycolipid-based oligosaccharide microarray system: preparation of NGLs and their noncovalent immobilization on nitrocellulose-coated glass slides for microarray analyses. Methods Mol Biol. 2012; 808:117–136. [PubMed: 22057521]
40. Stoll MS, Feizi T. Proceeding of the Beilstein Symposium on Glyco-Bioinformatics. 2009:123–140.
41. De Pauw B, et al. Revised definitions of invasive fungal disease from the European Organization for Research and Treatment of Cancer/Invasive Fungal Infections Cooperative Group and the National Institute of Allergy and Infectious Diseases Mycoses Study Group (EORTC/MSG) Consensus Group. Clin Infect Dis. 2008; 46:1813–1821. [PubMed: 18462102]
42. Kumar V, et al. Immunochip SNP array identifies novel genetic variants conferring susceptibility to candidaemia. Nature communications. 2014; 5:4675.
43. Johnson AD, et al. SNAP: a web-based tool for identification and annotation of proxy SNPs using HapMap. Bioinformatics. 2008; 24:2938–2939. [PubMed: 18974171]
44. Netea MG, et al. Aspergillus fumigatus evades immune recognition during germination through loss of toll-like receptor-4-mediated signal transduction. J Infect Dis. 2003; 188:320–326. [PubMed: 12854089]
45. Gray RT. A Class of K-Sample Tests for Comparing the Cumulative Incidence of a Competing Risk. Ann Stat. 1988; 16:1141–1154.
46. Scrucca L, Santucci A, Aversa F. Competing risk analysis using R: an easy guide for clinicians. Bone Marrow Transplant. 2007; 40:381–387. [PubMed: 17563735]
47. Leibundgut-Landmann S, Osorio F, Brown GD, Reis e Sousa C. Stimulation of dendritic cells via the dectin-1/Syk pathway allows priming of cytotoxic T-cell responses. Blood. 2008; 112:4971–4980. [PubMed: 18818389]

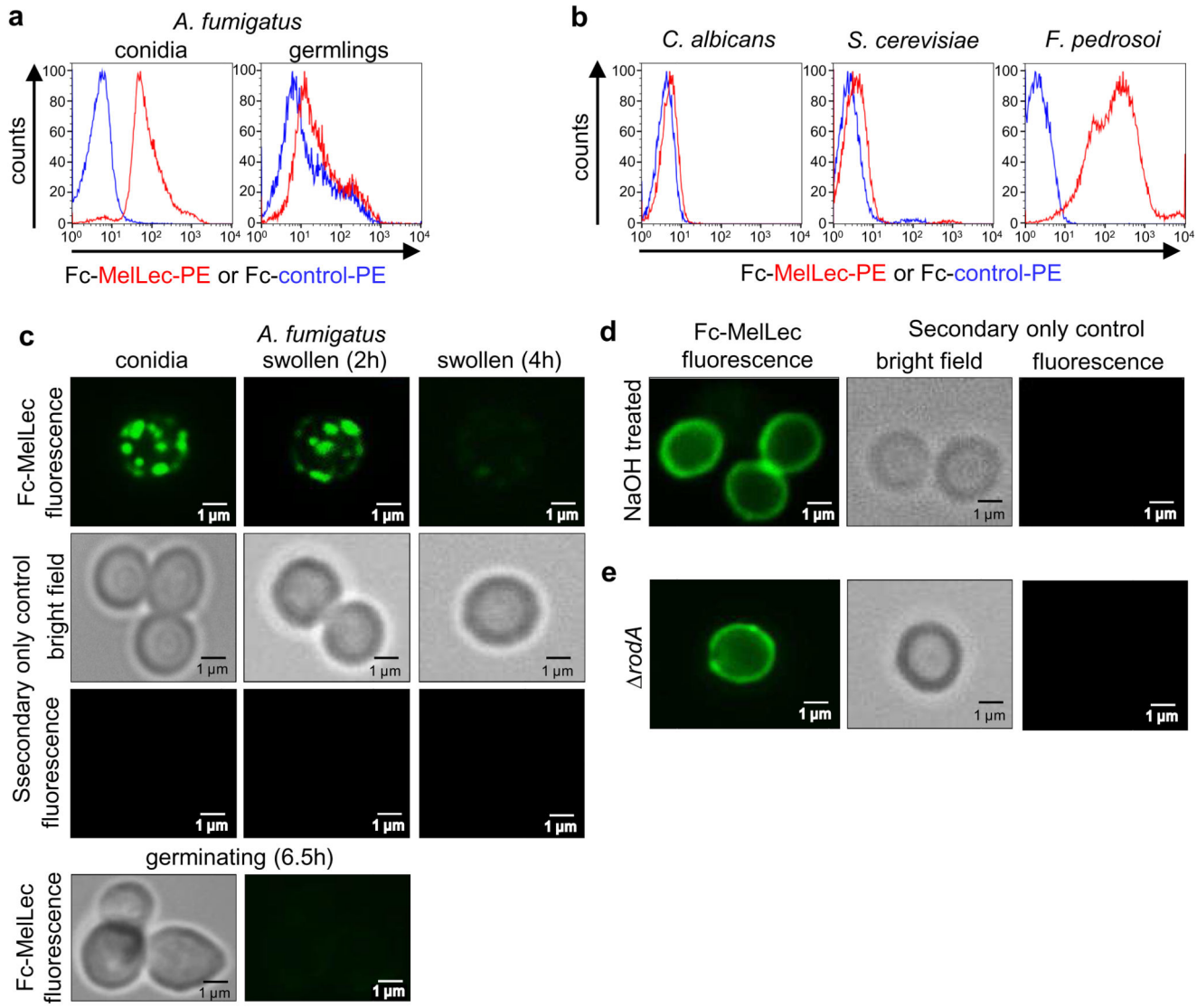

Figure 1. MelLec recognises selected fungi.

Representative histograms showing (**a**) *A. fumigatus* conidia and germlings (cultured for 8 h at 37°C), or (**b**) yeasts of *C. albicans* and *S. cerevisiae*, and conidia of *F. pedrosoi*, stained with Fc-MelLec or Fc-CLEC12b29 (Fc-control) and analysed by flow cytometry. Representative light microscope images and immunofluorescence micrographs using Fc-MelLec to detect ligands on *A. fumigatus* following conidial swelling and germination over time, as indicated (**c**), following treatment with 1M NaOH (**d**), and on rodlet-deficient (Δ*rodA*) conidia (**e**). **a**-**e**, Experiments were repeated at least 3 times independently, with similar results.

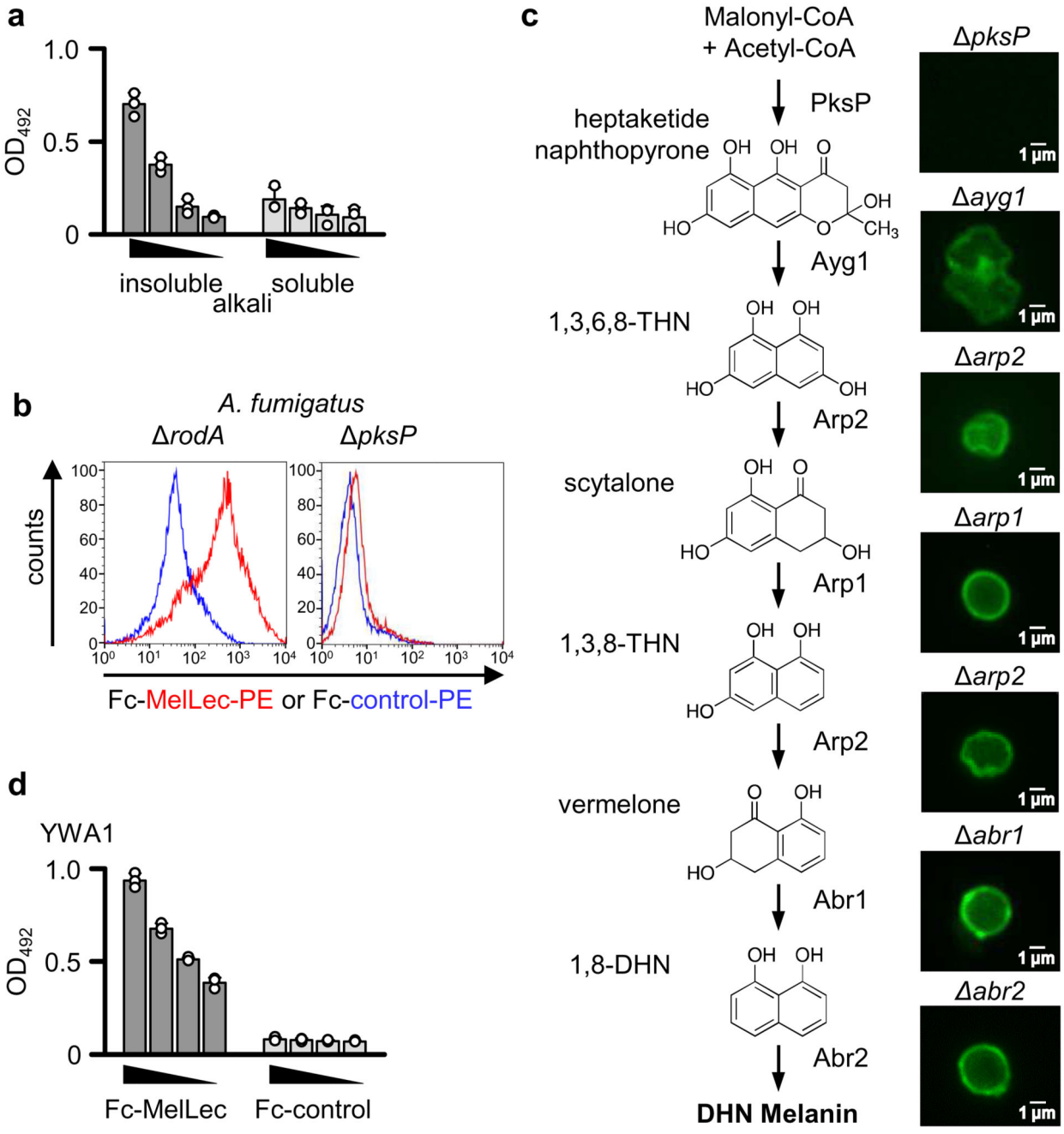

Figure 2. MelLec recognises DHN-melanin.

a, Detection of MelLec ligands in alkali insoluble or soluble *A. fumigatus* cell wall fractions by ELISA. Values show mean ± SD. **b**, Representative histograms showing Δ*rodA* or Δ*pksP* *A. fumigatus* conidia, stained with Fc-MelLec or Fc-CLEC12b (Fc-control) and analysed by flow cytometry. **c**, The biosynthetic pathway of DHN-melanin (left) and representative immunofluorescence micrographs using Fc-MelLec to detect ligands on *A. fumigatus* strains deficient in these enzymes (right). The conidial rodlet layer was removed with 1M NaOH prior to staining. **d**, Detection of YWA1 by Fc-MelLec and Fc-control by ELISA. Values

show mean ± SD. **a-d**, Experiments were repeated at least 3 times independently, with similar results.

Europe PMC Funders Author Manuscripts

Europe PMC Funders Author Manuscripts

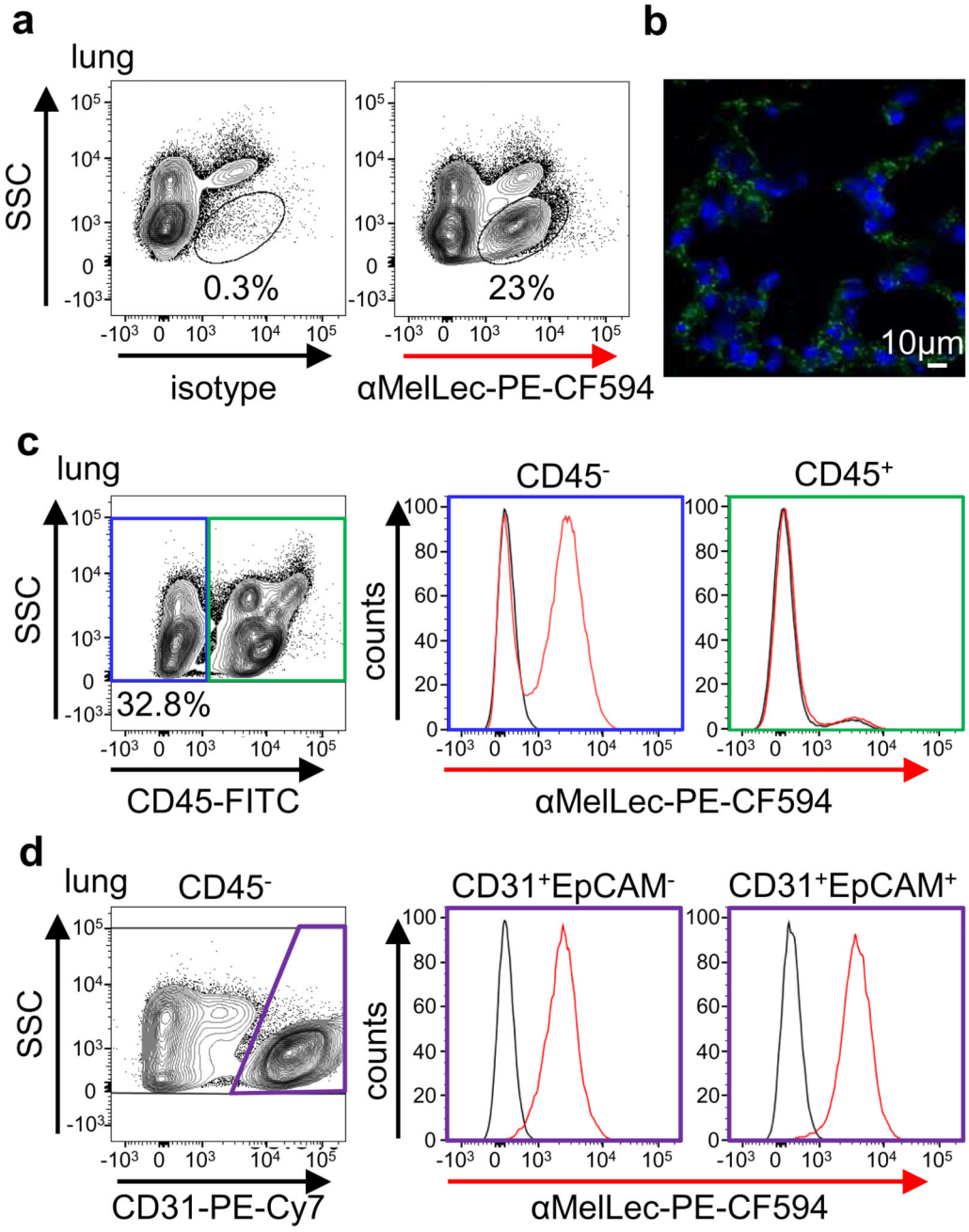

Figure 3. MelLec is expressed on non-myeloid cells in mouse.

a, Analysis of disaggregated lung tissue by flow cytometry with αMelLec. **b**, Immunofluorescence microscopy of lung tissue stained with αMelLec (green). Nuclei are stained with DAPI (blue). Flow cytometric analysis of MelLec expression on live $CD45^+$ and $CD45^-$ cells (**c**), and $CD45^-$ $CD31^+$ $EpCAM^-$ and $EpCAM^+$ cells (**d**) in the lung. **a**-**d**, Experiments were repeated at least 3 times independently, with similar results.

Europe PMC Funders Author Manuscripts

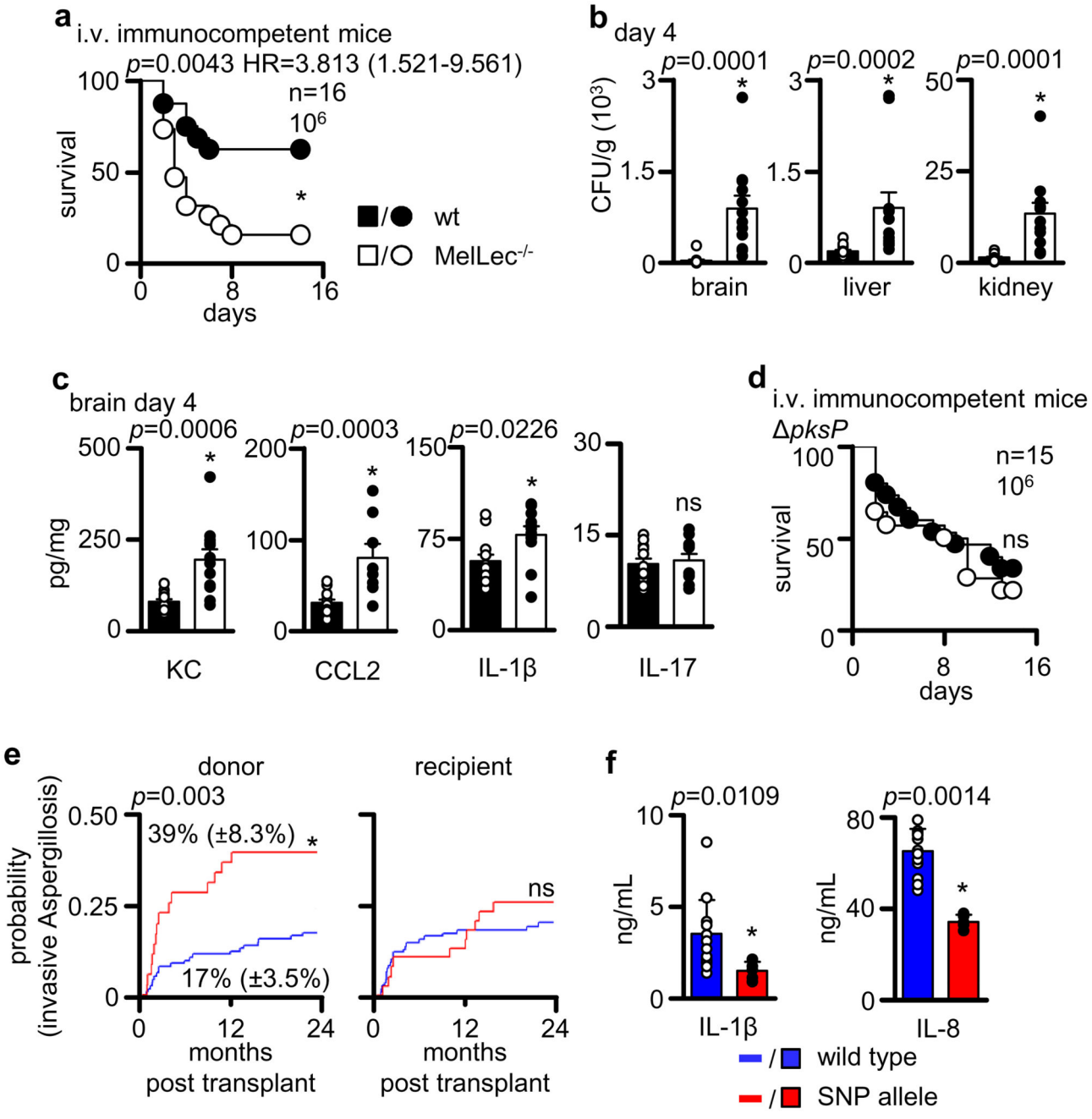

Figure 4. MelLec is required to prevent disseminated infection in mice and humans.

a, Survival of mice following intravenous (i.v.) infection with 10^6 *A. fumigatus* conidia (n=16 animals per group). Pooled data from two independent experiments, analysed by log-rank test. Tissue fungal burdens (**b**) and brain cytokine levels (**c**) of mice 4 days after i.v. infection with 10^6 *A. fumigatus* conidia (n=12 animals per group). **b-c**, Values shown are mean ± SEM of pooled data from two independent experiments, analysed by two-sided Mann-Whitney U test. **d**, Survival of mice following i.v. infection with 10^6 *ΔpksP A. fumigatus* conidia (n=15 animals per group). Pooled data from two independent

experiments, analysed by log-rank test. **e**, Cumulative incidence analysis of invasive aspergillosis after transplantation according to donor (wildtype, n=238 individuals; SNP allele, n=72 individuals) or recipient (wildtype, n=228 individuals; SNP allele, n=80 individuals) *CLEC1A* rs2306894 genotypes, analysed by two-sided Gray's test. **f**, Cytokine production in monocyte-derived macrophages, following stimulation with *A. fumigatus* conidia (wildtype, n=14 individuals; SNP allele, n=5 individuals). Values shown are mean ± SD, analysed by two-sided Mann-Whitney U test. *, p≤0.05; ns, not significant; HR, hazard ratio.

Europe PMC Funders Author Manuscripts